

Quantum Quasinormal Mode Theory for Dissipative Nano-Optics and Magnetodielectric Cavity Quantum Electrodynamics

Lars Meschede,¹ Daniel D. A. Clarke,¹ and Ortwin Hess^{1,2}

¹⁾*School of Physics and CRANN Institute, Trinity College Dublin, the University of Dublin, College Green, Dublin 2, Ireland*

²⁾*AMBER, SFI Research Centre for Advanced Materials and BioEngineering Research, Trinity College Dublin, the University of Dublin, College Green, Dublin 2, Ireland*

(*Electronic mail: ortwin.hess@tcd.ie)

(*Electronic mail: clarked5@tcd.ie)

(Dated: 24 July 2025)

The unprecedented pace of evolution in nanoscale architectures for cavity quantum electrodynamics (cQED) has posed crucial challenges for theory, where the quantum dynamics arising from the non-perturbative dressing of matter by cavity electric and magnetic fields, as well as the fundamentally non-hermitian character of the system are to be treated without significant approximation. The lossy electromagnetic resonances of photonic, plasmonic or magnonic nanostructures are described as quasinormal modes (QNMs), whose properties and interactions with quantum emitters and spin qubits are central to the understanding of dissipative nano-optics and magnetodielectric cQED. Despite recent advancements toward a fully quantum framework for QNMs, a general and universally accepted approach to QNM quantization for arbitrary linear media remains elusive. In this work, we introduce a unified theoretical framework, based on macroscopic QED and complex coordinate transformations, that achieves QNM quantization for a wide class of spatially inhomogeneous, dissipative (with possible gain components) and dispersive, linear, magnetodielectric resonators. The complex coordinate transformations equivalently convert the radiative losses into non-radiative material dissipation, and via a suitable transformation that reflects all the losses of the resonator, we define creation and annihilation operators that allow the construction of modal Fock states for the joint excitations of field-dressed matter. By directly addressing the intricacies of modal loss in a fully quantum theory of magnetodielectric cQED, our approach enables the exploration of modern, quantum nano-optical experiments utilizing dielectric, plasmonic, magnetic or hybrid cQED architectures, and paves the way towards a rigorous assessment of room-temperature quantum nanophotonic technologies without recourse to *ad hoc* quantization schemes.

I. INTRODUCTION

Cavity-mediated control and enhancement of light-matter interaction has become a pervasive paradigm in modern quantum science and technology. Already decades in maturity, the use of micro- and nanoscale, optical, dielectric resonators to both harness and manipulate the photonic properties of semiconductor quantum dots has enabled the exploration of fundamental cavity quantum electrodynamics (cQED) in the solid state^{1–3}, as well as a host of device applications ranging from high-performance, non-classical light sources and spin-photon interfaces to ultrafast, all-optical switching for integrated photonic quantum computation and networks^{4–6}. In stark contrast to their dielectric counterparts, plasmonic nanocavities offer the unique ability to confine light to extremely sub-wavelength scales and massively enhance local electromagnetic fields via their resonant surface plasmon modes, thereby constituting unique architectures for the exploration of light-matter interaction free from diffraction bounds⁷. Crucially, plasmonic resonators have ushered in an unprecedented era of room-temperature cQED at the nanoscale, facilitating access to the regime of strong coupling even at the profound limit of single molecular and quantum dot emitters under ambient conditions^{8–11}, and opening up

a compelling vista of potential applications in quantum nanotechnologies^{12,13}, extending from single-qubit coherent control¹⁴ and ultrafast single-photon emission^{15–17} to near-field multipartite entanglement generation^{18,19} and quantum sensing²⁰. In contrast to the electric dipole coupling between light and matter, cQED phenomena emerging from magnetic interactions have also been the subject of increasing attention. Leveraging collective microwave excitations of the spins in ferromagnetic and ferrimagnetic structures, the demonstration of such effects as photon-magnon and cavity-mediated magnon-qubit strong coupling^{21–24}, have established cavity (nano-)magnonics as an attractive paradigm²⁵, with interesting prospective applications in the engineering of synthetic gauge fields²⁶, cavity-mediated spin-photon interfaces at the nanoscale²⁷, and the realization of quantum networks of entangled spins.

As duly highlighted in the literature, the ability to describe the optical response of photonic, plasmonic or magnonic resonators and their interaction with quantum emitters (QEs) and spin qubits in terms of a small number of modes is of significant practical utility. A cavity mode formalism renders more transparent the physical attributes of light-matter interaction, allows one to isolate and quantify both radiative and non-radiative contributions to the observed dynamics, and aids de-

vice optimization towards particular applications. For ideal, closed cavities in the absence of material absorption (*i.e.*, hermitian systems), normal modes emerge with real eigenfrequencies (resonances), infinite lifetimes and which are orthonormal with respect to some scalar product. In practice, the dielectric microcavities of traditional semiconductor quantum optics (which feature very high quality factors) most closely approximate this scenario^{1,2}, but nevertheless, the notion remains ambiguous in general and cannot be applied without further considerations^{28,29}. The issue of decay is especially important for nanoplasmonic resonators, where Ohmic dissipation inherent to their metallic constituents and open-cavity radiation losses are essentially universal, but has also garnered interest in the context of magnonic cavity systems where dissipative coupling effects have been observed^{30,31}. Of course, these losses typically have a deleterious impact on the performance of schemes for quantum information processing¹², but could also be harnessed in order to engineer the functionality of quantum metamaterials and to promote novel veins of research in non-hermitian topological photonics or in the quantum thermodynamic facets of nanophotonic technologies. In all such cases, it is evidently desirable to capture in full the inherently dissipative character of the electromagnetic resonances.

To date, one of the most powerful and increasingly widespread approaches to this end has been quasinormal mode (QNM) theory^{29,32–39}. The QNMs are time-harmonic solutions to Maxwell's equations, satisfying suitable outgoing-wave boundary conditions (*e.g.*, the Silver-Müller radiation condition) and bearing complex eigenfrequencies, loss thus being accounted for as an intrinsic modal property. The imposition of a radiation condition ensures that light propagates away from the cavity (as expected for a leaky resonator), but in conjunction with the complex nature of their eigenfrequencies, gives rise to a mathematically and conceptually difficult property of QNMs, namely their spatial, exponential divergence at large distances from the resonator. More generally, the non-conservative nature of lossy cavity systems has raised a variety of non-trivial questions regarding a proper, mathematically rigorous formulation of normalization and orthogonality, alongside the matter of whether or not the QNMs truly form a complete set, and thus allow mode expansions for arbitrary electromagnetic field distributions. In spite of the challenges and ambiguities, classical QNM methodology has undergone significant advances in the last decade, including improved understanding of the formal aspects of the theory³⁹, techniques for computing the QNMs of arbitrary resonators^{37,38,40–43} and the release of general-purpose software⁴⁴, as well as successful applications to the calculation of generalized effective mode volumes^{28,29,41}, electromagnetic near- and far-field characteristics^{45–47}, Green's functions^{36,43}, enhanced spontaneous emission rates^{41,43,48,49} and even elastic Purcell factors in optomechanical systems⁵⁰.

Inevitably, a quantum description of lossy electromag-

netic modes is essential towards the fundamental study and understanding of quantum nanophotonic systems, including the statistics of photon, plasmon or magnon emission, polaritonic effects and the role of quantum fluctuations, as well as to facilitate rigorous quantification of key figures of merit for emerging quantum nanophotonic technologies. To date, most theoretical investigations of nanoscale cQED and spectroscopy (*e.g.*, surface-enhanced and electron energy loss spectroscopies) have relied on an *ad hoc* quantization protocol, in which the bosonic cavity mode is directly modeled as a quantum harmonic oscillator without formal, field-theoretic justification, while decay effects are incorporated via the relevant dissipators in a quantum master equation treatment, themselves derived from a phenomenological coupling to a bath of continuum modes^{51–53}. Recently however, significant progress was made with the introduction of a second quantization scheme for QNMs, enabling the construction of multiplasmon or multiphoton Fock states for arbitrary, three-dimensional (3D), dissipative and non-magnetic resonators⁵⁴. This approach has been elaborated and applied to a range of problems, such as concerning the limits of (phenomenological) dissipative Jaynes-Cummings models in plasmonic cQED, the performance of near-field-driven single-photon sources⁵⁵, the description of nonlinear cQED effects in hybrid metal-dielectric cavity systems⁵⁶ and coupled lossy and amplifying resonators⁵⁷. An important feature of these works is the regularization of the QNMs based on a Dyson equation formalism and a dual expansion scheme for the dyadic Green's function⁴³, which utilizes the unregularized modes for positions inside the resonator and regularized modes that are functions of real frequency for positions outside. Whilst the Dyson equation approach appears to yield an accurate representation for the Green's function outside the resonator volume and allows accurate calculation of the Purcell factor in this region for the studied systems⁴³, numerical computation of the regularized fields appears computationally intensive, and may even become intractable for more complex photonic cavity systems. Moreover, the formal justification for such a mode regularization technique remains elusive³⁹, and in particular, is based on an assumed completeness of the QNMs inside the resonator. Whilst this may apply to simple geometries, (*i.e.*, compact resonators in a homogeneous background medium), it is not guaranteed for more complex geometries, such as resonators on a substrate or waveguide-coupled resonator systems³⁹. Alternative quantization schemes for lossy and non-magnetic resonators have also emerged in the last few years, relying on a fitting of the spectral density of the electromagnetic environment⁵⁸ based on emitter-centered modes⁵⁹, or a transformation of the continuum of photonic eigenmodes into a discrete set of pseudomodes⁶⁰, where the latter offers the notable advantage of circumventing traditional reservoir approximations and can thereby capture non-Markovian effects in the dynamics of nanocavity-QE systems. Nevertheless, it remains desirable to formulate

a unified and numerically feasible methodology for describing the lossy resonances of arbitrary, linear, magnetodielectric systems, directly addressing such crucial issues as mode divergence, the identification of canonical field variables in the presence of both dielectric and magnetic media, and the calculation of key figures of merit for quantum nano-optical device applications on rigorous foundations. It is worth mentioning here that the quantization of QNMs and their coupling to QEs is similar to the reaction coordinate mapping of a (strongly-coupled) spin-boson model with a structured bath, described by a spectral density peaked around a certain frequency^{61,62}. In this method, the bosonic continuum is decomposed into a collective bosonic degree of freedom and a residual continuum, for which the interaction can be treated within the Markov approximation.

In this work, we present a unified theoretical framework that achieves QNM quantization for a wide class of 3D, spatially inhomogeneous, dissipative (with possible gain components) and dispersive, linear, magnetodielectric resonators. Our approach is based on a rigorously defined mode regularization and truncation of the spatial domain via exterior complex coordinate transformations, tantamount to perfectly matched layers (PMLs)^{39,63,64}. Harnessing established auxiliary-field eigenvalue techniques (or suitable generalizations thereof) with PMLs, a complete set of regularized modes can be ascertained, enabling the deployment of modal expansions for the dyadic Green's function and electromagnetic fields both inside and outside the resonator volume. The quantization of these modes is then treated in the formalism of macroscopic QED (mQED), facilitating the construction of discrete Fock states for the joint excitations of field-dressed matter in a manner that fully accounts for both radiative and non-radiative modal losses, and which provides the foundations for a quantum dynamic theory via quantum Langevin and master equations. Our present methodology attains unprecedented scope among quantum QNM techniques, offering a consolidated approach to the analysis of contemporary quantum nano-optical experiments utilizing dielectric, plasmonic, magnonic or hybrid cQED architectures, and paves the way towards a rigorous and numerically feasible assessment of the performance metrics for emerging, room-temperature-viable, quantum nanophotonic technologies without recourse to *ad hoc* quantization schemes.

The paper is organized as follows. § II briefly reviews the classical electromagnetic QNM theory and PML regularization, as well as the auxiliary-field eigenvalue technique that yields a complete set of orthonormalized modes, alongside useful formulae for time-domain analysis, in the commonly treated case of non-dispersive magnetic permeabilities. In § III, we discuss the theory of mQED in arbitrary, linear, magnetodielectric media; here, we quantize the modes by incorporating PML regularization in the formalism and defining bosonic modal operators in order to construct the corresponding Fock space. Using these operators, we derive an effective Lind-

blad master equation in § IV to describe the dynamics of the quantized modes and their coupling to QEs. In § V, we demonstrate the theory by investigating the spontaneous decay of a QE in a simple, 1D, half-open cavity, comparing our predictions with the semi-analytical results of an exact mQED treatment. Finally, we close the paper in § VI with some concluding remarks and perspectives.

II. CLASSICAL QNMS: REGULARIZATION, NORMALIZATION, AND COMPLETENESS BASED ON STRETCHED COORDINATES

A. Modal formulation of the scattering problem

In general, the electromagnetic resonances of a 3D, lossy and dispersive resonator are most rigorously treated as QNMs³⁹. We consider a system comprising a lossy resonator, contained in some compact region $\Omega_{\text{res}} \subset \mathbb{R}^3$ and embedded in some arbitrary linear material background described by a relative permittivity $\varepsilon_b(\mathbf{r}, \omega)$ and relative permeability $\mu_b(\mathbf{r}, \omega)$, while we denote the relative material parameters of the whole system by $\varepsilon(\mathbf{r}, \omega)$ and $\mu(\mathbf{r}, \omega)$. In general, the background does not need to be homogeneous and could, for example, contain a substrate or waveguides, as schematized in Fig. 1(a). The QNM electric and magnetic fields, \mathbf{E}_n and \mathbf{H}_n respectively, are defined as the time-harmonic solutions of the source-free Maxwell's equations,

$$\begin{bmatrix} 0 & -i\mu_0^{-1}\mu^{-1}(\mathbf{r}, \tilde{\omega}_n)\nabla \times \\ i\varepsilon_0^{-1}\varepsilon^{-1}(\mathbf{r}, \tilde{\omega}_n)\nabla \times & 0 \end{bmatrix} \begin{bmatrix} \mathbf{H}_n \\ \mathbf{E}_n \end{bmatrix} = \tilde{\omega}_n \begin{bmatrix} \mathbf{H}_n \\ \mathbf{E}_n \end{bmatrix}, \quad (1)$$

subject to an appropriate outgoing-wave boundary condition (note that we have assumed a time dependence of the form $e^{-i\omega t}$). Alternatively, the QNM problem in Eq. (1) can be formulated as an equation for the electric field only:

$$\nabla \times (\mu^{-1}(\mathbf{r}, \tilde{\omega}_n)\nabla \times \mathbf{E}_n) - \frac{\tilde{\omega}_n^2}{c^2}\varepsilon(\mathbf{r}, \tilde{\omega}_n)\mathbf{E}_n = 0. \quad (2)$$

In the case of a homogeneous background, one can use the Silver-Müller radiation condition, but in a more complex background the condition needs to be adjusted (see, for example, Refs.^{65,66}).

The QNM eigenfrequencies $\tilde{\omega}_n = \omega_n - i\gamma_n$ are generally complex in character by virtue of losses⁶⁷. Due to their exponential decay in time ($\gamma_n < 0$), the QNMs exponentially diverge in space at $|\mathbf{r}| \rightarrow \infty$ ³⁹. Moreover, since they satisfy an outgoing-wave condition, the QNMs can only be used to expand scattered fields. It is therefore natural to adopt a background-field formulation which splits the total field into $\mathbf{E}(\mathbf{r}, \omega) = \mathbf{E}_b(\mathbf{r}, \omega) + \mathbf{E}_{\text{sca}}(\mathbf{r}, \omega)$. Here, the background or incident field $\mathbf{E}_b(\mathbf{r}, \omega)$ satisfies Maxwell's

equations in the background medium,

$$\nabla \times (\mu_b^{-1} \nabla \times \mathbf{E}_b) - \frac{\omega^2}{c^2} \varepsilon_b \mathbf{E}_b = i\omega \mu_0 \mathbf{j}_b , \quad (3)$$

and could be a solution of the homogeneous equation or generated by some current density \mathbf{j}_b outside the resonator. Note that in the case of a non-trivial background geometry, scattering effects are already accounted for in the background part of the field, as sketched in Fig. 1(a). The scattered field $\mathbf{E}_{\text{sca}}(\mathbf{r}, \omega)$ then satisfies Maxwell's equations in the full system, see Fig. 1(b), with an effective current density

$$\begin{aligned} \nabla \times (\mu^{-1} \nabla \times \mathbf{E}_{\text{sca}}) - \frac{\omega^2}{c^2} \varepsilon \mathbf{E}_{\text{sca}} \\ = \frac{\omega^2}{c^2} \Delta \varepsilon \mathbf{E}_b - \nabla \times (\Delta \mu^{-1} \nabla \times \mathbf{E}_b) , \end{aligned} \quad (4)$$

where $\Delta \varepsilon = \varepsilon - \varepsilon_b$, $\Delta \mu^{-1} = \mu^{-1} - \mu_b^{-1}$ [$\text{supp}(\Delta \varepsilon(\cdot, \omega)/\Delta \mu^{-1}(\cdot, \omega)) \subseteq \Omega_{\text{res}}$], and the same outgoing-wave condition as for the QNMs.

With regard to the practical calculation of QNMs and the formulation of a modal theory, two problems arise that need to be addressed. Considering their calculation, an outgoing-wave condition is usually imposed as an asymptotic one for the fields at $|\mathbf{r}| \rightarrow \infty$, while in numerical calculations the domain must be truncated. Using the QNMs in an expansion of the scattered field \mathbf{E}_{sca} at real frequencies ω , it is apparent that this expansion cannot be valid at positions far away from the resonator due to their spatial divergence. In fact, it is known that the QNMs can only be used to expand the scattered field and the system's Green's function for positions inside the resonator, where they appear to form a complete set, provided that the resonator is defined by a discontinuity in the refractive index in space^{33,35,36}. However, even this is only true for trivial homogeneous backgrounds, and becomes generally invalid for more complex background geometries, such as the one sketched in Fig. 1, due to branch cuts of the Green's function^{37,39}. A general QNM expansion of the scattered field $\mathbf{E}_{\text{sca}}(\mathbf{r}, \omega)$ would thus have the form

$$\mathbf{E}_{\text{sca}}(\mathbf{r}, \omega) = \sum_n \alpha_n(\omega) \mathbf{E}_n(\mathbf{r}) + \mathbf{E}_{\text{nr}}(\mathbf{r}, \omega) , \quad (5)$$

in which $\mathbf{E}_{\text{nr}}(\mathbf{r}, \omega)$ is a non-resonant continuum contribution that prevents the formulation of a discrete QNM modal theory. Both challenges, the truncation of the domain and the incompleteness of the QNMs, can be addressed by using exterior complex coordinate transformations, or equivalently, PMLs.

PMLs were originally introduced in computational electrodynamics in order to simulate open boundaries⁶⁸. They are defined as material layers that surround a finite domain such that the dynamics therein are unaffected, *i.e.*, outgoing waves are transmitted, without reflection, into the PML region Ω_{PML} and are exponentially damped

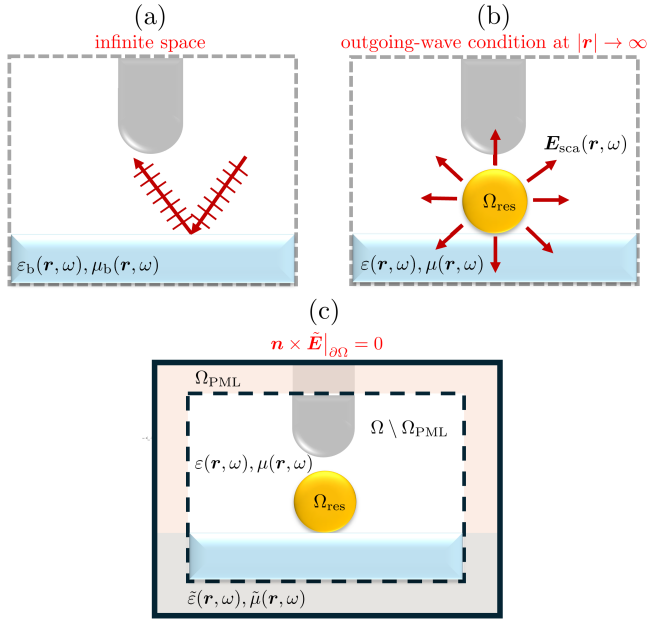


FIG. 1. Concept of the background-field formulation and the PML-based truncation of the domain used for QNM calculation, regularization and quantization. (a) Schematic of an example background, described by material parameters (ε_b, μ_b) , in which Maxwell's equations have to be satisfied by the background/incident field \mathbf{E}_b in the infinite space. The background can be non-trivial and contain substrates or waveguides. (b) The scattered-field problem in which Maxwell's equations have to be satisfied by \mathbf{E}_{sca} in the full geometry, including the resonator with compact domain Ω_{res} and containing the effective current density arising from \mathbf{E}_b . Suitable outgoing-wave conditions in the infinite space are applied. (c) The corresponding problem for \mathbf{E}_{sca} with PMLs imposed, in which the infinite space is truncated to a compact domain Ω . Using a complex coordinate transformation, which leaves the inner domain $\Omega \setminus \Omega_{\text{PML}}$ invariant and causes outgoing waves to be damped in Ω_{PML} , is equivalent to the introduction of an effective material $(\tilde{\varepsilon}(\mathbf{r}, \omega), \tilde{\mu}(\mathbf{r}, \omega))$. The damping of the outgoing waves effectively converts the outgoing-wave condition to a Dirichlet condition (perfect electrical conductor) at infinity, and due to the exponential nature of the damping, this boundary condition can very well be approximated using a finite truncated domain Ω and imposing the condition at $\partial\Omega$.

within them. The outgoing wave condition is thus effectively transformed into a Dirichlet (*i.e.*, perfect electrical conductor) boundary condition at $|\mathbf{r}| \rightarrow \infty$. Due to the fast exponential damping of the waves, it is a good approximation to consider PMLs with finite thickness only, so that the infinite space \mathbb{R}^3 has been effectively mapped to a finite domain Ω , in which we solve the scattered-field problem. This situation is sketched in Fig. 1(c). We denote the transformed material parameters of the mapped system by $(\tilde{\varepsilon}(\mathbf{r}, \omega), \tilde{\mu}(\mathbf{r}, \omega))$, whereas the inner domain $\Omega \setminus \Omega_{\text{PML}}$ is not affected by this transformation. When using PMLs, however, there are some limitations. In particular, the material parameters are required to be analytic functions in the directions perpendicular to

the PML boundaries (connected to the idea of PMLs as complex coordinate transformations), implying that the PMLs must be chosen in such a manner that waveguides enter with an angle of 90° , and periodic photonic crystal environments cannot be treated without further considerations⁶⁹.

We briefly review the formulation of PMLs in terms of complex coordinate transformations, focusing specifically on the case of Cartesian PMLs as sketched in Fig. 1(c), however, generalization is straightforward. For each coordinate x_i , the absorbing PML region is itself characterized by a (generally) coordinate-dependent absorption function $\sigma_i(x_i) \geq 0$ with $\text{supp}(\sigma_i) \subseteq \Omega_{\text{PML}}$. We can define the complex coordinate transformation corresponding to the PMLs as

$$x_i \mapsto \tilde{x}_i(x_i) = x_i + \frac{i}{\omega} \int^{x_i} dx'_i \sigma_i(x'_i), \quad (6)$$

under which any outgoing wave with wavevector component k_i becomes exponentially damped in the direction of x_i ,

$$\begin{aligned} \exp\{ik_i x_i\} &\mapsto \exp\{ik_i \tilde{x}_i(x_i)\} \\ &= e^{ik_i x_i - \frac{1}{c} \cos(\theta_i) \int^{x_i} dx'_i \sigma_i(x'_i)}, \end{aligned} \quad (7)$$

with $\cos(\theta_i) = ck_i/\omega$. PMLs were initially introduced to damp waves with real frequencies ω , but they can also be used to modify the behaviour of complex-frequency waves with $\tilde{\omega} = \omega - i\gamma$, *viz.*

$$|\exp\{ik_i \tilde{x}_i(x_i)\}| = e^{-\frac{1}{c} \cos(\theta_i) (\int^{x_i} dx'_i \sigma_i(x'_i) - \gamma x_i)}, \quad (8)$$

and can therefore be utilized for the computation of QNMs. Note that the wave is only damped if the expression in the brackets on the right-hand side is positive, *i.e.*, $\sigma_i(x_i)$ has to be chosen large enough. In theory, PMLs can be made arbitrarily attenuating by merely increasing $\sigma_i(x_i)$ and its thickness. As numerical calculations usually involve a discretization of space (via finite differences or finite elements), spurious numerical reflections occur, and one typically adopts a gradually increasing absorption profile $\sigma_i(x_i)$ to minimize them. By applying this transformation to all coordinates x_i , we obtain a coordinate transformation that damps all outgoing waves and has the Jacobian

$$J_{ij} = \frac{\partial \tilde{x}_i}{\partial x_j} = \left(1 + \frac{i}{\omega} \sigma_i(x_i)\right) \delta_{ij}. \quad (9)$$

By using the correspondence between coordinate transformations and effective materials in electrodynamics⁷⁰, Maxwell's equations with the material parameters (ε, μ) in the coordinates \tilde{x}_i can be rewritten in the real coordinates x_i with effective materials $(\tilde{\varepsilon}, \tilde{\mu})$ using the transformations

$$\tilde{\varepsilon} = \det(J) J^{-1} \varepsilon J^{-T}, \quad \tilde{\mu} = \det(J) J^{-1} \mu J^{-T}, \quad (10)$$

where $\det(J)$ is the determinant of the Jacobian. The transformed QNM eigenvalue problem, corresponding to Fig. 1(c), is thus given by

$$\begin{bmatrix} 0 & -i\mu_0^{-1} \tilde{\mu}^{-1}(\mathbf{r}, \tilde{\omega}_n) \nabla \times \\ i\varepsilon_0^{-1} \tilde{\varepsilon}^{-1}(\mathbf{r}, \tilde{\omega}_n) \nabla \times & 0 \end{bmatrix} \begin{bmatrix} \tilde{\mathbf{H}}_n \\ \tilde{\mathbf{E}}_n \end{bmatrix} = \tilde{\omega}_n \begin{bmatrix} \tilde{\mathbf{H}}_n \\ \tilde{\mathbf{E}}_n \end{bmatrix}. \quad (11)$$

The solutions of this transformed and PML-truncated eigenvalue problem are a discrete set of modes $\tilde{\mathbf{E}}_n(\mathbf{r})$ that can be grouped into QNM-like modes $\tilde{\mathbf{E}}_n^{\text{QNM}}(\mathbf{r})$, which are good approximations of the true QNMs of the system and do not depend on the parameters of the PMLs, and so-called numerical or PML modes $\tilde{\mathbf{E}}_n^{\text{PML}}(\mathbf{r})$ that depend sensitively on the PML parameters and which originate from the continuous non-resonant contribution in Eq. (5). Hence, by introducing finite-thickness PMLs, this background is effectively mapped to a discrete set of modes⁷¹. Since the operator in Eq. (11) is not hermitian, the completeness of these eigenmodes is not always guaranteed and we must further assume the absence of exceptional points where two eigenvectors coalesce. In this case, the PML-regularized scattered field $\tilde{\mathbf{E}}_{\text{sca}}$ can be expanded in this discrete set of modes,

$$\begin{aligned} \tilde{\mathbf{E}}_{\text{sca}}(\mathbf{r}, \omega) &= \sum_n \alpha_n^{\text{QNM}}(\omega) \tilde{\mathbf{E}}_n^{\text{QNM}}(\mathbf{r}) + \alpha_n^{\text{PML}}(\omega) \tilde{\mathbf{E}}_n^{\text{PML}}(\mathbf{r}) \\ &= \sum_n \alpha_n(\omega) \tilde{\mathbf{E}}_n(\mathbf{r}), \end{aligned} \quad (12)$$

where, henceforth, we shall not distinguish between the QNM-like and PML modes. Mathematically, they arise as a common set of solutions to the eigenvalue problem in Eq. (11), and should be treated on an equal footing for the purpose of further analysis.

In the context of non-dispersive magnetic permeabilities $\mu = \mu(\mathbf{r})$, Yan *et al.*³⁷ have developed an approach for rigorous QNM analysis of lossy resonators, relying on an auxiliary-field eigenvalue technique with PML regularization, within the framework of a finite-element analysis that enables efficient numerical calculations. Whilst the quantization scheme that we will discuss in § III can in principle be used for arbitrary dispersions of $(\tilde{\varepsilon}, \tilde{\mu})$, the approach of Yan *et al.* facilitates practical calculations in the important special cases of dielectric and plasmonic cQED, and formulae obtained within it can be used in the quantized theory for these cases as well (such as, for instance, the analytic excitation coefficients of the modes for an external driving field \mathbf{E}_b). As such, we will briefly discuss the key results of this approach in the next subsection.

B. Auxiliary-field eigenvalue technique

The non-linear nature of the eigenvalue problem in Eq. (11) for dispersive materials renders its numerical

solution difficult. The introduction of auxiliary fields in accordance with Yan *et al.*³⁷ aims to linearize the eigenvalue problem so that more conventional and efficient solvers can be leveraged. The permittivity distribution $\varepsilon(\mathbf{r}, \omega)$ is described using a position-dependent N -pole Drude-Lorentz model,

$$\varepsilon(\mathbf{r}, \omega) = \varepsilon_\infty(\mathbf{r}) - \varepsilon_\infty(\mathbf{r}) \sum_{l=1}^N \frac{\omega_{p,l}^2(\mathbf{r})}{\omega^2 - \omega_{0,l}^2(\mathbf{r}) + i\gamma_l(\mathbf{r})\omega},$$

in which $\gamma_l(\mathbf{r})$, $\omega_{p,l}(\mathbf{r})$ and $\omega_{0,l}(\mathbf{r})$ are damping rates, plasma and resonance frequencies pertaining to the l th pole, respectively. Dispersive PMLs like the one defined in Eq. (6) destroy the form of the Drude-Lorentz permittivity in Ω_{PML} and it is therefore common to use non-dispersive PMLs, in which the ω -dependence is replaced by a constant frequency ω_{PML} located within the frequency range of interest. These non-dispersive PMLs have the disadvantage that modes with lower frequency are less rapidly attenuated, thereby compromising the accuracy of the simulation. However, alternative auxiliary field methods can also be derived for arbitrary, rational dispersive permittivities (including dispersive PMLs), and studies with dispersive PMLs have been performed^{64,72}. For the non-dispersive PMLs, only $\varepsilon_\infty(\mathbf{r})$ in Eq. (II B) needs to be transformed to $\tilde{\varepsilon}_\infty(\mathbf{r})$, and auxiliary polarizations $\tilde{\mathbf{P}}_l$ and current densities $\tilde{\mathbf{J}}_l$ are defined for each pole, via

$$\tilde{\mathbf{P}}_l = -\frac{\varepsilon_0 \tilde{\varepsilon}_\infty(\mathbf{r}) \omega_{p,l}^2(\mathbf{r})}{\omega^2 - \omega_{0,l}^2(\mathbf{r}) + i\omega\gamma_l(\mathbf{r})} \tilde{\mathbf{E}}, \quad \tilde{\mathbf{J}}_l = -i\omega \tilde{\mathbf{P}}_l. \quad (13)$$

Treating the simple case of a single Drude-Lorentz pole ($N = 1$), we use these auxiliary fields to reformulate Eq. (11) as a linear eigenvalue problem, $\hat{\mathcal{H}}\tilde{\psi}_n = \tilde{\omega}_n \tilde{\psi}_n$, for an augmented eigenvector $\tilde{\psi}_n = [\tilde{\mathbf{H}}_n, \tilde{\mathbf{E}}_n, \tilde{\mathbf{P}}_n, \tilde{\mathbf{J}}_n]^T$, in which

$$\hat{\mathcal{H}} = \begin{bmatrix} 0 & -i(\mu_0 \tilde{\mu})^{-1} \nabla \times & 0 & 0 \\ i(\varepsilon_0 \tilde{\varepsilon}_\infty^{-1}) \nabla \times & 0 & 0 & -i(\varepsilon_0 \tilde{\varepsilon}_\infty)^{-1} \\ 0 & 0 & 0 & i \\ 0 & i\varepsilon_0 \tilde{\varepsilon}_\infty \omega_p^2 & -i\omega_0^2 & -i\gamma \end{bmatrix}. \quad (14)$$

The generalization to an arbitrary number N of poles is straightforward.

From the unconjugated form of the Lorentz reciprocity theorem, applied to the augmented system in Eq. (14), an orthogonality relation for the modes can be derived:

$$\int_{\Omega} d^3r \left(\varepsilon_0 \tilde{\varepsilon}_\infty(\mathbf{r}) \tilde{\mathbf{E}}_n \cdot \tilde{\mathbf{E}}_{n'} - \mu_0 \tilde{\mu}(\mathbf{r}) \tilde{\mathbf{H}}_n \cdot \tilde{\mathbf{H}}_{n'} \right. \\ \left. + \frac{\omega_0^2(\mathbf{r})}{\varepsilon_0 \tilde{\varepsilon}_\infty \omega_p^2(\mathbf{r})} \tilde{\mathbf{P}}_n \cdot \tilde{\mathbf{P}}_{n'} - \frac{1}{\varepsilon_0 \tilde{\varepsilon}_\infty(\mathbf{r}) \omega_p^2(\mathbf{r})} \tilde{\mathbf{J}}_n \cdot \tilde{\mathbf{J}}_{n'} \right) = \delta_{nn'}, \quad (15)$$

and their normalization condition can be readily written

as

$$\int_{\Omega} d^3r \left[\partial_{\omega} [\omega \varepsilon_0 \tilde{\varepsilon}(\mathbf{r}, \omega)]_{\omega=\tilde{\omega}_n} \tilde{\mathbf{E}}_n \cdot \tilde{\mathbf{E}}_n - \mu_0 \tilde{\mu}(\mathbf{r}) \tilde{\mathbf{H}}_n \cdot \tilde{\mathbf{H}}_n \right] \\ = 1. \quad (16)$$

It should be emphasized that the volume integration in these relations is performed over the entire computational domain Ω , including the PML regions Ω_{PML} , yet the normalization of the QNMs does not depend on the PML parameters³⁹. Although the orthogonality relation in this form can only be derived within the auxiliary-field eigenvalue approach, the normalization can also be used for materials with arbitrary dispersion and permeability, for which we would have to replace $\tilde{\mu} \rightarrow \partial_{\omega} [\omega \tilde{\mu}(\mathbf{r}, \omega)]$.

By defining the matrix

$$\hat{\mathcal{D}} = \text{diag} \left[-\mu_0 \tilde{\mu}, \varepsilon_0 \tilde{\varepsilon}_\infty, \frac{\omega_0^2}{\varepsilon_0 \tilde{\varepsilon}_\infty \omega_p^2}, \frac{-1}{\varepsilon_0 \tilde{\varepsilon}_\infty \omega_p^2} \right], \quad (17)$$

corresponding to the orthogonality relation in Eq. (15), the completeness relation can be written as

$$\sum_n \tilde{\psi}_n(\mathbf{r}') \otimes \tilde{\psi}_n^T(\mathbf{r}) \hat{\mathcal{D}}(\mathbf{r}) = \hat{\mathbf{I}} \delta(\mathbf{r} - \mathbf{r}'), \quad (18)$$

in which $\tilde{\psi}_n^T(\mathbf{r}) \hat{\mathcal{D}}$ are the left eigenvectors of $\hat{\mathcal{H}}^{37}$. Invoking the orthogonality and completeness properties, as well as the scattered-field formulation, we can derive analytic expressions for the modal excitation coefficients in Eq. (12):

$$\alpha_n(\omega) = \frac{\tilde{\omega}_n}{\tilde{\omega}_n - \omega} \varepsilon_0 \langle \tilde{\mathbf{E}}_n^* | \Delta \varepsilon(\mathbf{r}, \tilde{\omega}_n) | \mathbf{E}_b \rangle_{L^2(\Omega_{\text{res}})} \\ + \varepsilon_0 \langle \tilde{\mathbf{E}}_n^* | \varepsilon_b(\mathbf{r}, \omega) - \varepsilon_\infty(\mathbf{r}) | \mathbf{E}_b \rangle_{L^2(\Omega_{\text{res}})} \\ - \frac{\tilde{\omega}_n}{\tilde{\omega}_n - \omega} \mu_0 \langle \tilde{\mathbf{H}}_n^* | \Delta \mu(\mathbf{r}) | \mathbf{H}_b \rangle_{L^2(\Omega_{\text{res}})}, \quad (19)$$

in which $\langle \cdot | \cdot \rangle_{L^2(\Omega_{\text{res}})}$ is the standard complex L^2 -inner product over Ω_{res} . With these formulae, we can calculate the excitation coefficients in the frequency domain for arbitrary incident fields $\mathbf{E}_b(\mathbf{r}, \omega)$ through simple overlap integrals. A modal expansion as in Eq. (12) is also possible in the time domain with coefficients $\xi_n(t)$ related to $\alpha_n(\omega)$ via a Fourier transform and satisfying the equation

$$\frac{d\xi_n}{dt} = -i\tilde{\omega}_n \xi_n(t) + i\tilde{\omega}_n \varepsilon_0 \langle \tilde{\mathbf{E}}_n^* | \varepsilon(\tilde{\omega}_n) - \varepsilon_b | \mathbf{E}_b(t) \rangle \\ - \varepsilon_0 \langle \tilde{\mathbf{E}}_n^* | \varepsilon_b - \varepsilon_\infty | \frac{d}{dt} \mathbf{E}_b(t) \rangle - i\tilde{\omega}_n \mu_0 \langle \tilde{\mathbf{H}}_n^* | \Delta \mu | \mathbf{H}_b(t) \rangle \\ = -i\tilde{\omega}_n \xi_n(t) + D_n(t). \quad (20)$$

It is worth noting that although this auxiliary-field eigenvalue approach was originally introduced for systems with non-dispersive magnetic permeabilities $\mu(\mathbf{r})$, its generalization for media with strongly frequency-dependent permeabilities (as relevant for magnonic

cQED) may be feasible via the introduction of suitable auxiliary fields for the magnetic response. In the following, we assume that such a complete set of suitably regularized and normalized modes can be ascertained, and explore their quantization for arbitrary, linear, 3D, magnetodielectric systems.

III. QUANTIZATION OF THE REGULARIZED QUASINORMAL MODES

We now introduce a quantization scheme for the regularized QNMs of arbitrary, 3D, linear, dissipative (with possible gain components) and dispersive nanoresonators, as defined in § II. In our approach, we will quantize the eigenmodes of the PML-truncated domain in Eqs. (11) and (12). As already mentioned, this set of eigenmodes includes QNM-like and PML modes, which following our earlier remarks, shall simply be referred to as modes without further differentiation.

Similar to previous work^{54,56,57}, our approach is predicated on the formalism of mQED, which offers a phenomenological Green's function quantization scheme for electromagnetic fields in the presence of spatially inhomogeneous, lossy and dispersive media^{73–77}, later generalized for systems with gain^{78,79}. However, in order to facilitate a rigorous application of the theory, a brief discussion concerning some important prerequisites is warranted. The complex permittivity $\varepsilon(\mathbf{r}, \omega) = \varepsilon_r(\mathbf{r}, \omega) + i\varepsilon_i(\mathbf{r}, \omega)$ and inverse permeability $\mu^{-1}(\mathbf{r}, \omega) = \kappa(\mathbf{r}, \omega) = \kappa_r(\mathbf{r}, \omega) + i\kappa_i(\mathbf{r}, \omega)$ are required to satisfy the Kramers-Kronig relations (*i.e.*, they are analytic in the closed, upper-half, complex ω plane and $\zeta(\mathbf{r}, \omega) \rightarrow 1$ for $|\omega| \rightarrow \infty$ ($\zeta \in \{\varepsilon, \kappa\}$)). This is not really a requirement of the quantum theory, but arises from the physical necessity of causality. Furthermore, they should be reciprocal, $\zeta(\mathbf{r}, \omega) = \zeta^T(\mathbf{r}, \omega)$, and satisfy the reflection symmetry condition $\zeta_{ij}(\mathbf{r}, -\omega^*) = \zeta_{ij}^*(\mathbf{r}, \omega)$, which guarantees their reality in the time domain. These properties ensure that the fundamental QED commutation relations between the electric and magnetic field operators are maintained. If the material parameters $\zeta(\mathbf{r}, \omega)$ of the system are reciprocal, it readily follows from Eq. (10) that the PML-transformed parameters $\tilde{\zeta}(\mathbf{r}, \omega)$ are as well. It should be noted that there have been generalizations of mQED for the cases of non-reciprocal materials and materials with magnetoelectric crossing effects⁸⁰, which are, however, beyond the scope of this work.

When incorporating dispersive or non-dispersive PMLs in the quantization, two problems arise. For dispersive PMLs, it is easy to show from Eq. (10) and the Jacobian in Eq. (9) that the PML-transformed parameters $\tilde{\zeta}(\mathbf{r}, \omega)$ satisfy reflection symmetry, which preserves the important property that modes with $\Re(\tilde{\omega}_n) \neq 0$ always appear in pairs $(\tilde{\mathbf{E}}_\mu, \tilde{\omega}_\mu)$, $(\tilde{\mathbf{E}}_n^*, -\tilde{\omega}_n^*)$ and that all the modes have a non-positive imaginary part $\Im(\tilde{\omega}_n) \leq 0$. Due to the ω -dependence of the coordinate transformation, the material parameters have a pole at $\omega = 0$ and con-

sequently do not satisfy the Kramers-Kronig relations, (*i.e.*, they do not correspond to a causal medium). To resolve this issue, we could construct causal PMLs⁸¹ by making the replacement $\omega \rightarrow \omega + i\eta$ in Eq. (6) with a small $\eta > 0$, thereby shifting the pole into the lower, complex ω half-plane. Note that these causal PMLs also work, in principle, in the static case $\omega = 0$, due to the finite values of the transformed material parameters at this point⁸¹, whereas the usual PMLs fail and cannot be used to reproduce static modes⁸². However, we are only interested in the fields in the inner, unmapped domain $\Omega \setminus \Omega_{\text{PML}}$, and by using the properties of the Green's function we will show that the correct commutator is maintained within this region even if it is not in the PML region Ω_{PML} , so we expect that the use of PMLs as defined in Eq. (6) should suffice in most cases where static modes can be neglected. When using non-dispersive PMLs, the PML-transformed parameters no longer satisfy reflection symmetry, and since they do not afford the damping of waves with non-positive frequencies, the QNMs with $\Re(\tilde{\omega}_n) \leq 0$ are not correctly recovered and PML modes with $\Im(\tilde{\omega}_n) > 0$ occur, which would grow exponentially in time³⁹. In practice, one is often interested in the spectral response of a system only within a finite frequency interval $\Delta\omega$, in which case non-dispersive PMLs could be used provided that the contributions of the modes with $\Re(\tilde{\omega}_n) \leq 0$ are negligible in $\Delta\omega$. With the same argument, one can also justify the use of material parameters $\zeta(\mathbf{r}, \omega)$ or PMLs that do not satisfy the Kramers-Kronig relations (*e.g.*, non-dispersive and complex), provided that the true, physical parameters are sufficiently well approximated within $\Delta\omega$.

The formalism of mQED is based on the dyadic Green's function of the system, defined by

$$\nabla \times \tilde{\kappa} \nabla \times G(\mathbf{r}, \mathbf{r}', \omega) - \frac{\omega^2}{c^2} \tilde{\varepsilon} G(\mathbf{r}, \mathbf{r}', \omega) = \mathbf{I} \delta(\mathbf{r} - \mathbf{r}'). \quad (21)$$

If the system exhibits loss only, then the Green's function is analytic in the upper ω half-plane and has a set of discrete poles (corresponding to the QNMs), as well as possible branch cuts in the lower half-plane in the case of non-trivial background geometries. The introduction of gain components in the system shifts up the poles in the complex ω plane and a prerequisite to apply the theory for such active systems is that all the poles remain located in the lower half-plane. Again, this is not so much a fundamental limitation of the quantum theory but is, rather, a constraint on its range of validity for systems with linear amplification⁷⁹. The Green's function thus also satisfies the Kramers-Kronig relations, and besides that, reflection symmetry and the reciprocity $G(\mathbf{r}, \mathbf{r}', \omega) = G^T(\mathbf{r}', \mathbf{r}, \omega)$.

From Eq. (21), one can derive the useful relation

$$\Im(G(\mathbf{r}, \mathbf{r}', \omega)) = \frac{\omega^2}{c^2} \int_{\Omega} d^3s G^{\dagger}(\mathbf{s}, \mathbf{r}, \omega) \tilde{\epsilon}_i(\mathbf{s}, \omega) G(\mathbf{s}, \mathbf{r}', \omega) - \int_{\Omega} d^3s (\nabla \times G(\mathbf{s}, \mathbf{r}, \omega))^{\dagger} \tilde{\kappa}_i(\mathbf{s}, \omega) (\nabla \times G(\mathbf{s}, \mathbf{r}', \omega)) , \quad (22)$$

in which the curl operator has to be applied column-wise, and the real and imaginary parts of tensorial fields are defined as their hermitian and anti-hermitian parts, respectively, which reduce to the component-wise real and imaginary parts due to reciprocity. Note that although the integrals on the right-hand side have to be taken over the whole space, including the PML domain Ω_{PML} , the left-hand side does not depend on the PML parameters as long as $\mathbf{r}, \mathbf{r}' \in \Omega \setminus \Omega_{\text{PML}}$, given that the PMLs (ideally) do not affect the Green's function in the unmapped domain.

The second ingredient that we need to formulate the modal quantum theory is an expansion of the Green's function in terms of the modes in Eq. (11). By using a residue-decomposition approach, one can derive the expansion

$$G(\mathbf{r}, \mathbf{r}', \omega) = \sum_n A_n(\omega) \tilde{\mathbf{E}}_n(\mathbf{r}) \otimes \tilde{\mathbf{E}}_n(\mathbf{r}') , \quad (23)$$

with $A_n = \epsilon_0 c^2 / \omega(\tilde{\omega}_n - \omega)$ or $A_n = \epsilon_0 c^2 / \tilde{\omega}_n(\tilde{\omega}_n - \omega)$, where the non-uniqueness of the expansion stems from the overcompleteness of the set of modes³⁸.

In mQED, the frequency components of the quantized electric field operator $\hat{\mathbf{E}}(\mathbf{r}, \omega)$ satisfy the equation

$$\nabla \times \tilde{\kappa} \nabla \times \hat{\mathbf{E}}(\mathbf{r}, \omega) - \frac{\omega^2}{c^2} \tilde{\epsilon} \hat{\mathbf{E}}(\mathbf{r}, \omega) = i\omega \mu_0 \hat{\mathbf{j}}_F(\mathbf{r}, \omega) . \quad (24)$$

In the case of magnetodielectric materials with loss only, the noise/fluctuation current density $\hat{\mathbf{j}}_F(\mathbf{r}, \omega)$ introduced on the right-hand side, in accordance with the fluctuation-dissipation theorem, can be written as

$$\begin{aligned} \hat{\mathbf{j}}_F(\mathbf{r}, \omega) = & \omega \sqrt{\frac{\hbar \epsilon_0}{\pi}} \tilde{\epsilon}_{i,j}(\mathbf{r}, \omega) \hat{f}_{e,j}(\mathbf{r}, \omega) \mathbf{e}_j \\ & + \nabla \times \left(\sqrt{-\frac{\hbar}{\pi \mu_0}} \tilde{\kappa}_{i,j}(\mathbf{r}, \omega) \hat{f}_{m,j}(\mathbf{r}, \omega) \mathbf{e}_j \right) , \end{aligned} \quad (25)$$

in which we have used the Einstein summation convention and $\hat{f}_{\lambda,j}(\mathbf{r}, \omega)$ ($\hat{f}_{\lambda,j}^{\dagger}(\mathbf{r}, \omega)$) are bosonic annihilation (creation) operators of the joint (polaritonic) excitations of the field-dressed medium. The latter satisfy the commutation relation⁷⁴

$$[\hat{f}_{\lambda,i}(\mathbf{r}, \omega), \hat{f}_{\lambda',j}^{\dagger}(\mathbf{r}', \omega')] = \delta_{\lambda\lambda'} \delta_{ij} \delta(\mathbf{r} - \mathbf{r}') \delta(\omega - \omega') , \quad (26)$$

and diagonalize the material-field Hamiltonian:

$$\begin{aligned} \hat{H}_{\text{EM}} = & \int_{\Omega} d^3r \int_0^{\infty} d\omega \hbar \omega \left(\hat{f}_{e,j}^{\dagger}(\mathbf{r}, \omega) \hat{f}_{e,j}(\mathbf{r}, \omega) \right. \\ & \left. + \hat{f}_{m,j}^{\dagger}(\mathbf{r}, \omega) \hat{f}_{m,j}(\mathbf{r}, \omega) \right) . \end{aligned} \quad (27)$$

Note that in Eq. (25), we have assumed scalar material parameters $\zeta(\mathbf{r}, \omega)$ and Cartesian PMLs, for which the PML-transformed parameters are diagonal with $\tilde{\zeta}_{i,jj} = \tilde{\zeta}_{i,j}$. However, the analysis can easily be generalized for the non-diagonal case by replacing $\sqrt{\tilde{\zeta}_{i,j}(\mathbf{r}, \omega)}$ and the standard basis vectors \mathbf{e}_j by the eigenvalues and eigenvectors of the matrices $\Im(\zeta(\mathbf{r}, \omega))^{\frac{1}{2}}$, respectively (*i.e.*, by transforming to a system of principal axes). Explicitly, this would mean replacing Eq. (25) by

$$\begin{aligned} \hat{\mathbf{j}}_F(\mathbf{r}, \omega) = & \omega \sqrt{\frac{\hbar \epsilon_0}{\pi}} (\Im(\tilde{\epsilon}(\mathbf{r}, \omega))^{\frac{1}{2}} \cdot \hat{\mathbf{f}}_e(\mathbf{r}, \omega)) \\ = & \omega \sqrt{\frac{\hbar \epsilon_0}{\pi}} (\Im(\tilde{\epsilon}(\mathbf{r}, \omega))^{\frac{1}{2}} \mathbf{e}_i(\mathbf{r}, \omega) (\mathbf{e}_i^*(\mathbf{r}, \omega) \cdot \hat{\mathbf{f}}_e(\mathbf{r}, \omega))) \\ = & \omega \sqrt{\frac{\hbar \epsilon_0}{\pi}} (\Im(\tilde{\epsilon}(\mathbf{r}, \omega))^{\frac{1}{2}} \mathbf{e}_i(\mathbf{r}, \omega) \hat{\mathbf{f}}_e(\mathbf{r}, \omega)) , \end{aligned}$$

in which $(\Im(\tilde{\epsilon}(\mathbf{r}, \omega))^{\frac{1}{2}}$ are the eigenvalues of the matrix $\Im(\tilde{\epsilon}(\mathbf{r}, \omega))^{\frac{1}{2}}$ and $\mathbf{e}_i(\mathbf{r}, \omega)$ its eigenvectors, which are complete and orthonormal since $\Im(\tilde{\epsilon}(\mathbf{r}, \omega))^{\frac{1}{2}}$ is a hermitian matrix. Note that the eigenvectors are the same as those of the matrix $\Im(\tilde{\epsilon}(\mathbf{r}, \omega))$. The transformation would work in the same manner for the magnetic part, although the eigenvectors could be different. The Hamiltonian in Eq. (27) would have the same form in the transformed bosonic operators $\hat{f}_{e/m}(\mathbf{r}, \omega)$, as the scalar products are invariant under a change of basis.

The noise current defined in Eq. (25) stands in accordance with the fluctuation-dissipation theorem and ensures preservation of the fundamental commutation relations of the electric and magnetic fields. These formulae can also be derived from the canonical quantization of a microscopic model in which the electric and magnetic material responses are described using separate oscillator fields⁸³. From this perspective, it is clear that the Fock space corresponding to these bosonic variables describes not only the electromagnetic degrees of freedom, but also those of the material excitations.

In the case of materials exhibiting gain, the creation and annihilation operators interchange roles in the respective (finite) spatial and spectral regions. Eq. (25) must then be replaced by

$$\begin{aligned} \hat{\mathbf{j}}_F(\mathbf{r}, \omega) = & \omega \sqrt{\frac{\hbar \epsilon_0}{\pi}} |\tilde{\epsilon}_{i,j}(\mathbf{r}, \omega)| \mathbf{e}_j \left[\Theta(\tilde{\epsilon}_{i,j}(\mathbf{r}, \omega)) \hat{f}_{e,j}(\mathbf{r}, \omega) \right. \\ & \left. + \Theta(-\tilde{\epsilon}_{i,j}(\mathbf{r}, \omega)) \hat{f}_{e,j}^{\dagger}(\mathbf{r}, \omega) \right] \\ + & \nabla \times \left(\sqrt{\frac{\hbar}{\pi \mu_0}} |\tilde{\kappa}_{i,j}(\mathbf{r}, \omega)| \mathbf{e}_j \left[\Theta(-\tilde{\kappa}_{i,j}(\mathbf{r}, \omega)) \hat{f}_{m,j}(\mathbf{r}, \omega) \right. \right. \\ & \left. \left. + \Theta(\tilde{\kappa}_{i,j}(\mathbf{r}, \omega)) \hat{f}_{m,j}^{\dagger}(\mathbf{r}, \omega) \right] \right) , \end{aligned} \quad (28)$$

and the (normal-ordered) Hamiltonian in Eq. (27) by

$$\hat{H}_{\text{EM}} = \int_{\Omega} d^3r \int_0^{\infty} d\omega \hbar\omega \quad (29)$$

$$\cdot \left(\text{sgn}(\tilde{\varepsilon}_{i,j}(\mathbf{r}, \omega)) \hat{f}_{e,j}^{\dagger}(\mathbf{r}, \omega) \hat{f}_{e,j}(\mathbf{r}, \omega) \right. \\ \left. + \text{sgn}(-\tilde{\kappa}_{i,j}(\mathbf{r}, \omega)) \hat{f}_{m,j}^{\dagger}(\mathbf{r}, \omega) \hat{f}_{m,j}(\mathbf{r}, \omega) \right).$$

Note that excitations in the gain regions have a negative-energy contribution to the Hamiltonian. These expressions can again be derived from a microscopic model using inverted oscillator fields in the gain regions⁸⁴. However, it is worth underlining that the expressions in Eqs. (25) and (28) cannot be derived from a generalized phenomenological quantization scheme that allows for general non-local material responses described by a conductivity tensor, whenever the permittivity and permeability are spatially inhomogeneous^{77,79}. Since these expressions can be motivated from a microscopic model and provide analytic results for arbitrary magnetodielectric media, we will make use of them in this paper.

By using the definition of the Green's function in Eq. (21), the total electric field operator in the Schrödinger picture can now be written as

$$\hat{\mathbf{E}}(\mathbf{r}, \omega) = i\mu_0 \int_0^{\infty} d\omega \omega \int_{\Omega} d^3s G(\mathbf{r}, \mathbf{s}, \omega) \mathbf{j}_F(\mathbf{s}, \omega) + \text{h.c.} \\ = \hat{\mathbf{E}}^{(+)}(\mathbf{r}) + \hat{\mathbf{E}}^{(-)}(\mathbf{r}), \quad (30)$$

where $\hat{\mathbf{E}}^{(\pm)}(\mathbf{r})$ are the positive/negative frequency parts. By using Eq. (28) and the identity in Eq. (22), we can ascertain the commutator of the electric field operator:

$$\left[\hat{\mathbf{E}}_i^{(+)}(\mathbf{r}), \hat{\mathbf{E}}_j^{(-)}(\mathbf{r}') \right] \\ = \frac{\hbar\mu_0}{\pi} \int_0^{\infty} d\omega \omega^2 \int d^3s \\ \cdot \left[\frac{\omega^2}{c^2} G_{im}^{\dagger}(\mathbf{s}, \mathbf{r}, \omega) \tilde{\varepsilon}_{i,m}(\mathbf{s}, \omega) G_{mj}(\mathbf{s}, \mathbf{r}', \omega) \right. \\ \left. - (\nabla \times G(\mathbf{s}, \mathbf{r}, \omega))^{\dagger}_{im} \tilde{\kappa}_{i,m}(\mathbf{s}, \omega) (\nabla \times G(\mathbf{s}, \mathbf{r}', \omega))_{mj} \right] \\ = \frac{\hbar\mu_0}{\pi} \int_0^{\infty} d\omega \omega^2 \Im(G(\mathbf{r}, \mathbf{r}', \omega))_{ij}, \quad (31)$$

where the latter equation shows that the commutator is not affected by the PMLs for $\mathbf{r}, \mathbf{r}' \in \Omega \setminus \Omega_{\text{PML}}$. By invoking the first equality and the Green's function expansion in Eq. (23), we can expand the commutator in terms of the modes:

$$\left[\hat{\mathbf{E}}_i^{(+)}(\mathbf{r}), \hat{\mathbf{E}}_j^{(-)}(\mathbf{r}') \right] = \sum_{n,n'} P_{nn'} \tilde{\mathbf{E}}_{n,i}(\mathbf{r}) \tilde{\mathbf{E}}_{n',j}^*(\mathbf{r}'), \quad (32)$$

with

$$P_{nn'} = \frac{\hbar\mu_0}{\pi} \int_0^{\infty} d\omega \omega^2 \int d^3s A_n(\omega) A_{n'}^*(\omega) \quad (33)$$

$$\cdot \left[\frac{\omega^2}{c^2} \tilde{\mathbf{E}}_n(\mathbf{s}) \tilde{\varepsilon}_i(\mathbf{s}, \omega) \tilde{\mathbf{E}}_{n'}^*(\mathbf{s}) \right. \\ \left. - (\nabla \times \tilde{\mathbf{E}}_n(\mathbf{s})) \tilde{\kappa}_i(\mathbf{s}, \omega) (\nabla \times \tilde{\mathbf{E}}_{n'}^*(\mathbf{s})) \right].$$

These integrals describe the losses of the modes. Ultimately, our aim is to develop a suitable modal expansion of the electric field operator. As we consider general, anisotropic, magnetodielectric systems which could exhibit electric and magnetic losses in distinct spatial/frequency regions, we start by decomposing the QNM operators in electric/magnetic and loss/gain components; we thus introduce the four operators ($\hat{\xi}_{n,e,L}$, $\hat{\xi}_{n,e,G}$, $\hat{\xi}_{n,m,L}$, $\hat{\xi}_{n,m,G}$) for each mode and expand the electric field operator in the form

$$\hat{\mathbf{E}}(\mathbf{r}) = \sum_n \tilde{\mathbf{E}}_n(\mathbf{r}) (\hat{\xi}_{n,e,L} + \hat{\xi}_{n,e,G}^{\dagger} + \hat{\xi}_{n,m,L} + \hat{\xi}_{n,m,G}^{\dagger}) \\ + \text{h.c.} \\ = \hat{\mathbf{E}}^{(+)}(\mathbf{r}) + \hat{\mathbf{E}}^{(-)}(\mathbf{r}), \quad (34)$$

in which the modal operators can be expressed through the continuous bosonic variables:

$$\hat{\xi}_{n,e,L/G}^{(\dagger)} = i\mu_0 \int_0^{\infty} d\omega \omega^2 A_n(\omega) \int d^3r \theta(\pm \tilde{\varepsilon}_{i,j}(\mathbf{r}, \omega)) \\ \sqrt{\frac{\hbar\omega_0}{\pi}} |\tilde{\varepsilon}_{i,j}(\mathbf{r}, \omega)| \mathbf{e}_j \cdot \tilde{\mathbf{E}}_n(\mathbf{r}) \hat{f}_{e,j}^{\dagger}(\mathbf{r}, \omega), \quad (35)$$

$$\hat{\xi}_{n,m,L/G}^{(\dagger)} = i\mu_0 \int_0^{\infty} d\omega \omega A_n(\omega) \int d^3r \theta(\mp \tilde{\kappa}_{i,j}(\mathbf{r}, \omega)) \\ \sqrt{\frac{\hbar}{\pi\mu_0}} |\tilde{\kappa}_{i,j}(\mathbf{r}, \omega)| \mathbf{e}_j \cdot (\nabla \times \tilde{\mathbf{E}}_n(\mathbf{r})) \hat{f}_{m,j}^{\dagger}(\mathbf{r}, \omega). \quad (36)$$

Note that the hermitian conjugates of the gain operators $\hat{\xi}_{n,e/m,G}$ have to be used in the expansion of the positive-frequency part of the electric field, in order to reproduce the correct commutation relation as given in Eq. (32). Although they are hermitian conjugates of modal operators, they still behave like superpositions of positive-frequency excitations ($\propto e^{-i\omega t}$), as can be seen from Eqs. (35) and (36), and the Heisenberg equations for the continuous variables $\hat{f}_{e/m,j}(\mathbf{r}, \omega)$ in the gain regions with the Hamiltonian of Eq. (29). This is analogous to the approach in Ref.⁵⁷. In our case, however, we have included the PMLs into the quantization, which always exhibit gain. In the presence of gain materials, the vacuum correlation

function of the electric field would be given by

$$\begin{aligned} & \langle \hat{E}_i(\mathbf{r}) \hat{E}_j(\mathbf{r}') \rangle \\ &= \frac{\hbar\mu_0}{\pi} \int_0^\infty d\omega \omega^2 \int d^3r \\ & \cdot \left[\frac{\omega^2}{c^2} G_{im}^\dagger(\mathbf{s}, \mathbf{r}, \omega) |\tilde{\varepsilon}_{i,m}(\mathbf{s}, \omega)| G_{mj}(\mathbf{s}, \mathbf{r}', \omega) \right. \\ & \left. - (\nabla \times G(\mathbf{s}, \mathbf{r}, \omega))_{im}^\dagger |\tilde{\kappa}_{i,m}(\mathbf{s}, \omega)| (\nabla \times G(\mathbf{s}, \mathbf{r}', \omega))_{mj} \right]. \end{aligned} \quad (37)$$

Due to the moduli of the material parameters in this formula, the identity in Eq. (22) cannot be used to express the correlation function in terms of the imaginary part of the Green's function, which must be taken into account when, for example, calculating QE decay rates⁸⁵ or Casimir(-Polder) forces⁸⁶. In our approach, this implies that the presence of gain components in the PMLs would affect the correlation function due to induced fluctuations and thus the quantum dynamics, as they would, for example, affect the spontaneous decay of a QE. This means that in order to obtain the correct correlation function of the real system without contributions from the PMLs, we have to eliminate these fluctuations attributable to the gain components of the PMLs from our modal theory. To achieve this, we redefine the gain and loss operators in Eqs. (35) and (36) by including the gain components of the PML region Ω_{PML} in the loss operators:

$$\begin{aligned} \hat{\xi}_{n,e,L} &= +i\mu_0 \int_0^\infty d\omega \omega^2 A_n(\omega) \int_\Omega d^3r \left[\theta(\tilde{\varepsilon}_{i,j}(\mathbf{r}, \omega)) \right. \\ & \left. \sqrt{\frac{\hbar\varepsilon_0}{\pi} |\tilde{\varepsilon}_{i,j}(\mathbf{r}, \omega)|} \mathbf{e}_j \cdot \tilde{\mathbf{E}}_n(\mathbf{r}) \hat{f}_{e,j}(\mathbf{r}, \omega) \right] \\ & + i\mu_0 \int_0^\infty d\omega \omega^2 A_n(\omega) \int_{\Omega_{\text{PML}}} d^3r \left[\theta(-\tilde{\varepsilon}_{i,j}(\mathbf{r}, \omega)) \right. \\ & \left. \sqrt{\frac{\hbar\varepsilon_0}{\pi} |\tilde{\varepsilon}_{i,j}(\mathbf{r}, \omega)|} \mathbf{e}_j \cdot \tilde{\mathbf{E}}_n(\mathbf{r}) \hat{f}_{e,j}^\dagger(\mathbf{r}, \omega) \right] \\ &= \hat{\xi}_{n,e,L} + \hat{\xi}_{n,e,\text{PML}}^\dagger, \end{aligned} \quad (38)$$

$$\begin{aligned} \hat{\xi}_{n,e,G}^\dagger &= i\mu_0 \int_0^\infty d\omega \omega^2 A_n(\omega) \int_{\Omega \setminus \Omega_{\text{PML}}} d^3r \left[\theta(-\tilde{\varepsilon}_{i,j}(\mathbf{r}, \omega)) \right. \\ & \left. \sqrt{\frac{\hbar\varepsilon_0}{\pi} |\tilde{\varepsilon}_{i,j}(\mathbf{r}, \omega)|} \mathbf{e}_j \cdot \tilde{\mathbf{E}}_n(\mathbf{r}) \hat{f}_{e,j}^\dagger(\mathbf{r}, \omega) \right], \end{aligned} \quad (39)$$

$$\begin{aligned} \hat{\xi}_{n,m,L} &= +i\mu_0 \int_0^\infty d\omega \omega A_n(\omega) \int_\Omega d^3r \left[\theta(-\tilde{\kappa}_{i,j}(\mathbf{r}, \omega)) \right. \\ & \left. \sqrt{\frac{\hbar}{\pi\mu_0} |\tilde{\kappa}_{i,j}(\mathbf{r}, \omega)|} \mathbf{e}_j \cdot (\nabla \times \tilde{\mathbf{E}}_n(\mathbf{r})) \hat{f}_{m,j}(\mathbf{r}, \omega) \right] \\ & + i\mu_0 \int_0^\infty d\omega \omega A_n(\omega) \int_{\Omega_{\text{PML}}} d^3r \left[\theta(\tilde{\kappa}_{i,j}(\mathbf{r}, \omega)) \right. \\ & \left. \sqrt{\frac{\hbar}{\pi\mu_0} |\tilde{\kappa}_{i,j}(\mathbf{r}, \omega)|} \mathbf{e}_j \cdot (\nabla \times \tilde{\mathbf{E}}_n(\mathbf{r})) \hat{f}_{m,j}^\dagger(\mathbf{r}, \omega) \right] \\ &= \hat{\xi}_{n,m,L} + \hat{\xi}_{n,m,\text{PML}}^\dagger, \end{aligned} \quad (40)$$

$$\begin{aligned} \hat{\xi}_{n,m,G}^\dagger &= +i\mu_0 \int_0^\infty d\omega \omega A_n(\omega) \int_{\Omega \setminus \Omega_{\text{PML}}} d^3r \left[\theta(\tilde{\kappa}_{i,j}(\mathbf{r}, \omega)) \right. \\ & \left. \sqrt{\frac{\hbar}{\pi\mu_0} |\tilde{\kappa}_{i,j}(\mathbf{r}, \omega)|} \mathbf{e}_j \cdot (\nabla \times \tilde{\mathbf{E}}_n(\mathbf{r})) \hat{f}_{m,j}^\dagger(\mathbf{r}, \omega) \right]. \end{aligned} \quad (41)$$

These loss operators thus satisfy the commutation relations

$$\begin{aligned} \left[\hat{\xi}_{n,e,L}, \hat{\xi}_{n',e,L}^\dagger \right] &= \frac{\hbar\mu_0}{\pi} \int_0^\infty d\omega \omega^2 A_n(\omega) A_{n'}^*(\omega) \\ & \left[+ \int_\Omega d^3r \theta(\tilde{\varepsilon}_{i,j}(\mathbf{r}, \omega)) \frac{\omega^2}{c^2} |\tilde{\varepsilon}_{i,j}(\mathbf{r}, \omega)| E_{n,j}(\mathbf{r}) E_{n',j}^*(\mathbf{r}) \right. \\ & \left. - \int_{\Omega_{\text{PML}}} d^3r \theta(-\tilde{\varepsilon}_{i,j}(\mathbf{r}, \omega)) \frac{\omega^2}{c^2} |\tilde{\varepsilon}_{i,j}(\mathbf{r}, \omega)| E_{n,j}(\mathbf{r}) E_{n',j}^*(\mathbf{r}) \right] \\ &= \tilde{P}_{nn'}^{\text{e,L}} - \tilde{P}_{n'n}^{\text{e,PML}} = P_{nn'}^{\text{e,L}}, \end{aligned} \quad (42)$$

$$\begin{aligned} \left[\hat{\xi}_{n,m,L}, \hat{\xi}_{n',m,L}^\dagger \right] &= P_{nn'}^{\text{m,L}} = \frac{\hbar\mu_0}{\pi} \int_0^\infty d\omega \omega^2 A_n(\omega) A_{n'}^*(\omega) \\ & \left[+ \int_\Omega d^3r \theta(-\tilde{\kappa}_{i,j}(\mathbf{r}, \omega)) |\tilde{\kappa}_{i,j}(\mathbf{r}, \omega)| \right. \\ & \left. (\nabla \times \tilde{\mathbf{E}}_n(\mathbf{r}))_j (\nabla \times \tilde{\mathbf{E}}_{n'}^*(\mathbf{r}))_j \right. \\ & \left. - \int_{\Omega_{\text{PML}}} d^3r \theta(\tilde{\kappa}_{i,j}(\mathbf{r}, \omega)) |\tilde{\kappa}_{i,j}(\mathbf{r}, \omega)| \right. \\ & \left. (\nabla \times \tilde{\mathbf{E}}_n(\mathbf{r}))_j (\nabla \times \tilde{\mathbf{E}}_{n'}^*(\mathbf{r}))_j \right] \\ &= \tilde{P}_{nn'}^{\text{m,L}} - \tilde{P}_{n'n}^{\text{m,PML}} = P_{nn'}^{\text{e,L}}, \end{aligned} \quad (43)$$

and the gain operators satisfy

$$\begin{aligned} \left[\hat{\xi}_{n,e,G}, \hat{\xi}_{n',e,G}^\dagger \right] &= P_{nn'}^{\text{e,G}} = \frac{\hbar\mu_0}{\pi} \int_0^\infty d\omega \omega^2 A_n^*(\omega) A_{n'}(\omega) \\ & \int_{\Omega \setminus \Omega_{\text{PML}}} d^3r \theta(-\tilde{\varepsilon}_{i,j}(\mathbf{r}, \omega)) \frac{\omega^2}{c^2} |\tilde{\varepsilon}_{i,j}(\mathbf{r}, \omega)| E_{n,j}^*(\mathbf{r}) E_{n',j}(\mathbf{r}) \end{aligned} \quad (44)$$

$$\begin{aligned} \left[\hat{\xi}_{n,m,G}, \hat{\xi}_{n',m,G}^\dagger \right] = P_{nn'}^{m,G} = \frac{\hbar\mu_0}{\pi} \int_0^\infty d\omega \omega^2 A_n^*(\omega) A_{n'}(\omega) \\ \int_{\Omega \setminus \Omega_{\text{PML}}} d^3r \theta(\tilde{\kappa}_{i,j}(\mathbf{r}, \omega)) |\tilde{\kappa}_{i,j}(\mathbf{r}, \omega)| \\ (\nabla \times \mathbf{E}_n^*(\mathbf{r}))_j (\nabla \times \mathbf{E}_{n'}(\mathbf{r}))_j \end{aligned} \quad (45)$$

All the other commutators vanish due to the bosonic commutation relations of the variables $\hat{f}_\lambda(\mathbf{r}, \omega)$ and the distinct loss/gain regions. Since the commutation relations of these modal operators are non-bosonic, we have to apply symmetrization transformations separately to the electric/magnetic and loss/gain components in order to ascertain bosonic modal operators^{54,87}:

$$\hat{a}_{n,e/m,L/G} = \left(P^{e/m,L/G} \right)_{nn'}^{-\frac{1}{2}} \hat{\xi}_{n',e/m,L/G}. \quad (46)$$

Note that the matrices of the new loss operators $P_{nn'}^{e/m,L}$ now have negative contributions from the gain components of the PMLs, as can be seen in Eqs. (42) and (43). However, as the loss is much more dominant in the PMLs, we will still assume that these matrices are positive-definite, ensuring the existence of the inverses and square roots. These new operators $\hat{a}_{n,e/m,L/G}$ satisfy bosonic commutation relations:

$$\left[\hat{a}_{n,\lambda,X}, \hat{a}_{n',\lambda',X'}^\dagger \right] = \delta_{nn'} \delta_{\lambda\lambda'} \delta_{XX'}, \quad (47)$$

with $\lambda = e, m$ and $X = L, G$. Due to the different commutators, these operators correspond to differently symmetrized modes, which are superpositions of the original modes $\tilde{\mathbf{E}}_n(\mathbf{r})$:

$$\tilde{\mathbf{E}}_{n,\lambda,L}^{\text{sym}}(\mathbf{r}) = (P^{\lambda,L})_{n'n}^{\frac{1}{2}} \tilde{\mathbf{E}}_{n'}(\mathbf{r}), \quad (48)$$

$$\tilde{\mathbf{E}}_{n,\lambda,G}^{\text{sym}}(\mathbf{r}) = (P^{\lambda,G})_{nn'}^{\frac{1}{2}} \tilde{\mathbf{E}}_{n'}(\mathbf{r}). \quad (49)$$

The electric field operator can then be written as

$$\hat{\mathbf{E}}^{(+)}(\mathbf{r}) = \sum_{n,\lambda} \tilde{\mathbf{E}}_{n,\lambda,L}^{\text{sym}}(\mathbf{r}) \hat{a}_{n,\lambda,L} + \tilde{\mathbf{E}}_{n,\lambda,G}^{\text{sym}}(\mathbf{r}) \hat{a}_{n,\lambda,G}^\dagger. \quad (50)$$

From the definitions of the modal operators in Eqs. (38)–(41), it is apparent that the loss operators do not have the same vacuum state $|0\rangle$ as the continuum operators $\hat{f}_\lambda(\mathbf{r}, \omega)$, as we have included the gain part of the PMLs in the loss operators ($\hat{a}_{n,e/m,L} |0\rangle \neq 0$). Nevertheless, we adopt it as the vacuum state of the modal operators ($\hat{a}_{n,e/m,L} |0\rangle = 0$) and use it to construct a modal bosonic Fock space \mathcal{F} , in which the k -photon Fock states can be constructed from $|0\rangle$ in the usual manner:

$$|k_{n,\lambda,X}\rangle = \frac{1}{\sqrt{k_{n,\lambda,X}!}} \left(\hat{a}_{n,\lambda,X}^\dagger \right)^k |0\rangle. \quad (51)$$

The commutator calculated from Eq. (50) is clearly equal to the one calculated from the exact theory as $P_{nn'} =$

$P_{nn'}^{\text{e,L}} + P_{nn'}^{\text{m,L}} - P_{n'n}^{\text{e,G}} - P_{n'n}^{\text{m,G}}$. Furthermore, if we calculate the vacuum correlation function from Eq. (50) in the constructed Fock space, we now obtain

$$\begin{aligned} & \langle \hat{E}_i(\mathbf{r}) \hat{E}_j(\mathbf{r}') \rangle \\ &= \sum_{n,n'} (P_{nn'}^{\text{e,L}} + P_{nn'}^{\text{m,L}} + P_{n'n}^{\text{e,G}} + P_{n'n}^{\text{m,G}}) \tilde{E}_{n,i}(\mathbf{r}) \tilde{E}_{n',j}^*(\mathbf{r}') \\ &= \frac{\hbar\mu_0}{\pi} \int_0^\infty d\omega \omega^2 \left[\right. \\ & \quad \int_{\Omega \setminus \Omega_{\text{PML}}} \frac{\omega^2}{c^2} G_{im}^\dagger(\mathbf{s}, \mathbf{r}, \omega) |\tilde{\varepsilon}_{i,m}(\mathbf{s}, \omega)| G_{mj}(\mathbf{s}, \mathbf{r}', \omega) \\ & \quad + (\nabla \times G(\mathbf{s}, \mathbf{r}, \omega))_{im}^\dagger |\tilde{\kappa}_{i,m}(\mathbf{s}, \omega)| (\nabla \times G(\mathbf{s}, \mathbf{r}', \omega))_{mj} \\ & \quad + \int_{\Omega_{\text{PML}}} \frac{\omega^2}{c^2} G_{im}^\dagger(\mathbf{s}, \mathbf{r}, \omega) \tilde{\varepsilon}_{i,m}(\mathbf{s}, \omega) G_{mj}(\mathbf{s}, \mathbf{r}', \omega) \\ & \quad \left. - (\nabla \times G(\mathbf{s}, \mathbf{r}, \omega))_{im}^\dagger \tilde{\kappa}_{i,m}(\mathbf{s}, \omega) (\nabla \times G(\mathbf{s}, \mathbf{r}', \omega))_{mj} \right]. \end{aligned} \quad (52)$$

Note that in contrast to the exact vacuum correlation function in the presence of the PMLs [see Eq. (37)], the moduli of the material parameters do not appear in the integral over the PML region. By using the identity in Eq. (22), we can write the correlation function as

$$\begin{aligned} & \langle \hat{E}_i(\mathbf{r}) \hat{E}_j(\mathbf{r}') \rangle = \frac{\hbar\mu_0}{\pi} \int_0^\infty d\omega \omega^2 \left[\Im(G(\mathbf{r}, \mathbf{r}', \omega))_{ij} \right. \\ & + 2 \int_{\Omega \setminus \Omega_{\text{PML}}} d^3r \frac{\omega^2}{c^2} \theta(-\tilde{\varepsilon}_{i,m}(\mathbf{r}, \omega)) \\ & \quad \cdot G_{im}^\dagger(\mathbf{s}, \mathbf{r}, \omega) |\tilde{\varepsilon}_{i,m}(\mathbf{s}, \omega)| G_{mj}(\mathbf{s}, \mathbf{r}', \omega) \\ & \quad + \theta(\tilde{\kappa}_{i,m}(\mathbf{r}, \omega)) \\ & \quad \cdot (\nabla \times G(\mathbf{s}, \mathbf{r}, \omega))_{im}^\dagger |\tilde{\kappa}_{i,m}(\mathbf{s}, \omega)| (\nabla \times G(\mathbf{s}, \mathbf{r}', \omega))_{mj} \left. \right], \end{aligned} \quad (53)$$

showing that it is not altered by the presence of the PMLs and reflects the correlation function of the real system without PMLs. Our modal theory thus reproduces the correct commutators and vacuum correlation functions of the exact theory. The magnetic field operator can be expanded using the same bosonic modal operators:

$$\hat{\mathbf{B}}^{(+)}(\mathbf{r}) = \sum_{n,\lambda} \tilde{\mathbf{B}}_{n,\lambda,L}^{\text{sym}}(\mathbf{r}) \hat{a}_{n,\lambda,L} + \tilde{\mathbf{B}}_{n,\lambda,G}^{\text{sym}}(\mathbf{r}) \hat{a}_{n,\lambda,G}^\dagger, \quad (54)$$

with

$$\tilde{\mathbf{B}}_{n,\lambda,L}^{\text{sym}}(\mathbf{r}) = (P^{\lambda,L})_{n'n}^{\frac{1}{2}} \frac{1}{i\tilde{\omega}_{n'}} \nabla \times \tilde{\mathbf{E}}_{n'}(\mathbf{r}), \quad (55)$$

$$\tilde{\mathbf{B}}_{n,\lambda,G}^{\text{sym}}(\mathbf{r}) = (P^{\lambda,G})_{nn'}^{\frac{1}{2}} \frac{1}{i\tilde{\omega}_{n'}} \nabla \times \tilde{\mathbf{E}}_{n'}(\mathbf{r}). \quad (56)$$

It should be emphasized that so far, we have treated the most general case of linear, magnetodielectric media, for which the permittivities and permeabilities can exhibit gain contributions, and introduced four operators per mode. In the following, we will discuss three important

simplifications and special cases in which the complexity of the modal description can be reduced considerably.

1. Combination of electric/magnetic operators

The electric and magnetic operators can in principle always be combined as $\hat{\xi}_{n,X} = \hat{\xi}_{n,e,X} + \hat{\xi}_{n,m,X}$, even if the electric and magnetic responses exhibit gain in distinct spatial/spectral regions. In this case only two operators per mode are needed, which satisfy the commutation relations

$$[\hat{\xi}_{n,X}, \hat{\xi}_{n',X}^\dagger] = P_{nn'}^X = P_{nn'}^{e,X} + P_{nn'}^{m,X}. \quad (57)$$

After the corresponding symmetrization, similar to Eq. (46), the expanded electric field operator would read

$$\hat{\mathbf{E}}^{(+)}(\mathbf{r}) = \sum_n \tilde{\mathbf{E}}_{n,L}^{\text{sym}}(\mathbf{r}) \hat{a}_{n,L} + \tilde{\mathbf{E}}_{n,G}^{\text{sym}}(\mathbf{r}) \hat{a}_{n,G}^\dagger, \quad (58)$$

in which the symmetrized modes are defined as in Eqs. (48) and (49), with the replacements $P^{\lambda,X} \rightarrow P^X$. Even though this simplification can always be made, we introduced distinct electric/magnetic modal operators above as they may provide additional physical information in the case of magnetodielectric systems, where for instance, the modes might be hybrid in character with plasmonic and magnonic components. When studying the decay of QEs in such systems, the splitting of the modal operators would also provide information on whether the QEs dominantly excite plasmonic or magnonic polaritons, as the operators $\hat{\xi}_{n,e/m,X}$ are superpositions of electric/magnetic, polaritonic, matter-field excitations $\hat{f}_{e/m}(\mathbf{r}, \omega)$.

2. Combination of gain/loss operators

If we combine the gain and loss operators as $\hat{\xi}_{n,\lambda} = \hat{\xi}_{n,\lambda,L} + \hat{\xi}_{n,\lambda,G}^\dagger$, they would satisfy the commutation relations

$$[\hat{\xi}_{n,\lambda}, \hat{\xi}_{n',\lambda}^\dagger] = P_{nn'}^\lambda = P_{nn'}^{\lambda,L} - P_{n'n}^{\lambda,G}, \quad (59)$$

just as we have seen when we included the gain components of the PMLs in the loss operators of Eqs. (42) and (43). However, caution is required at this point, because the vacuum fluctuations and the corresponding pumping of the modes due to the gain components of the resonator have a physical influence that generally cannot be neglected, and which becomes clear in the effective master equation derived in § III. As discussed in Ref.⁵⁷, two conditions must be met for the gain and loss operators to be combined. Firstly, the combined matrices $P_{nn'}^\lambda$ must be positive-definite, which is required for the symmetrization of the modal operators. Secondly, as already pointed out when treating the gain components of the PMLs, the combined operators $\hat{\xi}_{n,\lambda}$ do not have the same vacuum state $|0\rangle$ as the continuous variables $\hat{f}_\lambda(\mathbf{r}, \omega)$. Applying the modal number operators (without the contributions from the PML gain components) to the vacuum state leads to $\sum_n \hat{a}_{n,\lambda}^\dagger \hat{a}_{n,\lambda} |0\rangle = \sum_n n_{n,\lambda}^0 |0\rangle$ with $\sum_n n_{n,\lambda}^0 = \text{Tr}\{P^{\lambda,G*}(P^\lambda)^{-1}\}$. Consequently, the

vacuum state of the complete system can only be used approximately as a vacuum state of the modal Fock space if $\sum_n n_{n,\lambda}^0 \ll 1$, which holds whenever the losses in the system dominate the gain (*i.e.*, $P_{nn}^{\lambda,L} \gg P_{nn}^{\lambda,G}$) and the off-diagonal elements $P_{nn'}^{\lambda,G}$ are small. In this case, the expanded electric field operator would read

$$\hat{\mathbf{E}}^{(+)}(\mathbf{r}) = \sum_n \tilde{\mathbf{E}}_{n,e}^{\text{sym}}(\mathbf{r}) \hat{a}_{n,e} + \tilde{\mathbf{E}}_{n,m}^{\text{sym}}(\mathbf{r}) \hat{a}_{n,m}, \quad (60)$$

in which the symmetrized modes are as defined in Eq. (48) with the replacement $P^{\lambda,L} \rightarrow P^\lambda$. Note that in this approximation, quantum effects due to the vacuum fluctuations caused by the presence of the gain regions are neglected, however, they still influence the dynamics as their presence alters the modes and the Green's function of the system.

3. Combination of all four operators

If the electric/magnetic modal operators are combined and we additionally combine the gain/loss operators, only one operator per mode $\hat{\xi}_n = \hat{\xi}_{n,e,L} + \hat{\xi}_{n,m,L} + \hat{\xi}_{n,e,G}^\dagger + \hat{\xi}_{n,m,G}^\dagger$ is needed, satisfying the commutation relations

$$[\hat{\xi}_n, \hat{\xi}_{n'}^\dagger] = P_{nn'} = P_{nn'}^{e,L} + P_{nn'}^{m,L} - P_{n'n}^{e,G} - P_{n'n}^{m,G}, \quad (61)$$

and leading to the expansion

$$\hat{\mathbf{E}}^{(+)}(\mathbf{r}) = \sum_n \tilde{\mathbf{E}}_n^{\text{sym}}(\mathbf{r}) \hat{a}_n, \quad (62)$$

in which the symmetrized modes are defined as in Eq. (48) with the replacement $P^{\lambda,L} \rightarrow P$. Note that the combined gain and loss matrices $P_{nn'}^X = P_{nn'}^{e,X} + P_{nn'}^{m,X}$ have to satisfy the same conditions as discussed in the last paragraph.

It is also worth mentioning that in our approach, the limit of lossless/gainless materials, (*i.e.*, $\zeta_i \rightarrow 0$), can be taken from the beginning, since we map the problem onto a compact domain $\Omega \subset \mathbb{R}^3$. This means that in this case, we can interchange the limit and the integration in the symmetrization matrix elements $P_{nn'}^{\lambda,L}$, and consequently only the PML region Ω_{PML} contributes, which corresponds to the radiation loss in Ref.⁸⁸.

IV. EFFECTIVE LINDBLAD MASTER EQUATION

In this section, we derive an effective Lindblad master equation for the electromagnetic modes and the additional coupling to a QE, described as a two-level system (TLS). We will start by considering the dynamics of the modes only in the most general scenario, in which they are characterized by the operators $\hat{a}_{n,\lambda,X}$. In the Heisenberg picture, the dynamics of each modal operator is determined by the Heisenberg equation of motion

$d\hat{O}/dt = i[\hat{H}, \hat{O}]/\hbar$, leading to⁵⁷

$$\begin{aligned} \frac{d\hat{a}_{n,\lambda,L}}{dt} = \frac{i}{\hbar} [\hat{H}_{\text{eff}}, \hat{a}_{n,\lambda,L}] - (\tilde{\chi}_{nn'}^{\lambda,L,-} - \tilde{\chi}_{nn'}^{\lambda,PML,-}) \hat{a}_{n',\lambda,L} \\ + \hat{F}_{n,\lambda,L}(t) + \hat{F}_{n,\lambda,PML}^\dagger(t), \end{aligned} \quad (63)$$

$$\frac{d\hat{a}_{n,\lambda,G}}{dt} = \frac{i}{\hbar} [\hat{H}_{\text{eff}}, \hat{a}_{n,\lambda,G}] - \chi_{nn'}^{\lambda,G,-} \hat{a}_{n,\lambda,G} + \hat{F}_{n,\lambda,G}(t), \quad (64)$$

with an effective Hamiltonian

$$\hat{H}_{\text{eff}} = \hbar \chi_{nn'}^{\lambda,L,+} \hat{a}_{n,\lambda,L}^\dagger \hat{a}_{n',\lambda,L} - \hbar \chi_{nn'}^{\lambda,G,+} \hat{a}_{n,\lambda,G}^\dagger \hat{a}_{n',\lambda,G}, \quad (65)$$

and the coupling matrices

$$\chi_{nn'}^{\lambda,X,+} = \frac{1}{2} (P^{\lambda,X})_{nn''}^{-\frac{1}{2}} (\tilde{\omega}_{n''} + \tilde{\omega}_{n'''}^*) P_{n''n'''}^{\lambda,X} (P^{\lambda,X})_{n'''n'}^{-\frac{1}{2}}, \quad (66)$$

$$\tilde{\chi}_{nn'}^{\lambda,L,-} = \frac{i}{2} (P^{\lambda,L})_{nn''}^{-\frac{1}{2}} (\tilde{\omega}_{n''} - \tilde{\omega}_{n'''}^*) \tilde{P}_{n''n'''}^{\lambda,L} (P^{\lambda,L})_{n'''n'}^{-\frac{1}{2}}, \quad (67)$$

$$\tilde{\chi}_{nn'}^{\lambda,PML,-} = \frac{i}{2} (P^{\lambda,L})_{nn''}^{-\frac{1}{2}} (\tilde{\omega}_{n''} - \tilde{\omega}_{n'''}^*) \tilde{P}_{n''n'''}^{\lambda,PML} (P^{\lambda,L})_{n'''n'}^{-\frac{1}{2}}, \quad (68)$$

$$\chi_{nn'}^{\lambda,G,-} = \frac{i}{2} (P^{\lambda,G})_{nn''}^{-\frac{1}{2}} (\tilde{\omega}_{n''} - \tilde{\omega}_{n'''}^*) P_{n''n'''}^{\lambda,G} (P^{\lambda,G})_{n'''n'}^{-\frac{1}{2}}. \quad (69)$$

The $\hat{F}_{n,\lambda,L/G/PML}(t)$ are additional operator terms that still depend on the continuous variables $\hat{f}_\lambda(\mathbf{r}, \omega)$, and which cannot be expressed simply in terms of the modal operators. From the classical QNM theory, it is clear that the amplitudes of the freely evolving modes are oscillating with the complex frequencies $\tilde{\omega}_n$, as can be seen in Eq. (20), meaning the expectation values of the modal operators should satisfy $\langle \hat{\xi}_{n,\lambda,L}(t) \rangle = \langle \hat{\xi}_{n,\lambda,L}(0) \rangle e^{-i\tilde{\omega}_n t}$ and $\langle \hat{\xi}_{n,\lambda,G/PML}(t) \rangle = \langle \hat{\xi}_{n,\lambda,G/PML}(0) \rangle e^{+i\tilde{\omega}_n^* t}$. From that requirement, it is clear that $\langle \hat{F}_{n,\lambda,L/G/PML}^{(\dagger)}(t) \rangle = 0$. Furthermore, the peaked structure was factored out in the spectral representations of the operators $\hat{F}_{n,\lambda,L/G/PML}(t)$ due to terms of the form $(\tilde{\omega}_\mu - \omega) A_\mu(\omega) = \varepsilon_0 c^2 / \tilde{\omega}_\mu$. We thus make a Markov approximation and treat them as white quantum noise forces induced by the dissipation/gain and that ensure the preservation of the commutation relations. This procedure is similar to the reaction coordinate mapping, in which the coupling of a TLS to a structured bath having a strongly peaked spectral density is mapped to an interaction with a discrete mode and a residual continuum that can then be treated within the Markov approximation^{61,62}. Note that in the equation for the modal loss operators $\hat{a}_{n,\lambda,L}$ two noise forces $\hat{F}_{m,\lambda,L/PML}^{(\dagger)}$ appear that counteract the loss and gain terms described by $\tilde{\chi}_{nn'}^{\lambda,L/PML,-}$, caused by the overall loss in the system and the gain components of the

PMLs, which we have included in the loss operators [see Eq. (38)]. In the equation for the modal gain operators $\hat{a}_{n,\lambda,G}$, only one noise force $\hat{F}_{m,\lambda,G}$ appears that counteracts a loss term proportional to $\chi_{nn'}^{\lambda,G,-}$. The pumping of the modes due to the gain components of the resonator are described by negative-energy contributions in the effective Hamiltonian of Eq. (65), associated to the separate modal gain operators.

By invoking a quantum analogue of Itô-Stratonovich calculus, following the same procedure as in Refs.^{54,57,89}, an effective Markovian master equation, corresponding to the Heisenberg-Langevin equations in Eqs. (63) and (64), can be obtained in the form

$$\begin{aligned} \frac{d\rho}{dt} = -\frac{i}{\hbar} [\hat{H}_{\text{eff}}, \rho] + \tilde{\chi}_{nn'}^{\lambda,L,-} \mathcal{D}_{nn'}^{\lambda,L} \rho + \chi_{nn'}^{\lambda,G,-} \mathcal{D}_{nn'}^{\lambda,G} \rho \\ + \tilde{\chi}_{nn'}^{\lambda,PML,-} \mathcal{D}_{nn'}^{\lambda,PML} \rho, \end{aligned} \quad (70)$$

with the same effective Hamiltonian as in Eq. (65) and the Lindblad dissipators

$$\mathcal{D}_{nn'}^{\lambda,X} \rho = 2 \hat{a}_{n',\lambda,X} \rho \hat{a}_{n,\lambda,X}^\dagger - \{\rho, \hat{a}_{n,\lambda,X}^\dagger \hat{a}_{n',\lambda,X}\}, \quad (71)$$

$$\mathcal{D}_{nn'}^{\lambda,PML} \rho = 2 \hat{a}_{n,\lambda,L}^\dagger \rho \hat{a}_{n',\lambda,L} - \{\rho, \hat{a}_{n',\lambda,L} \hat{a}_{n,\lambda,L}^\dagger\}, \quad (72)$$

where the terms $\mathcal{D}_{nn'}^{\lambda,X} \rho$ describe dissipation and $\mathcal{D}_{nn'}^{\lambda,PML} \rho$ the incoherent pumping by the gain components of the PMLs.

This is the effective master equation that governs the quantum dynamics of the modes for the most general case, featuring decomposed electric/magnetic modal operators. Note that the loss/gain present in the system necessitates a symmetrization of the modes and consequently induces a coupling between the bosonic modes in both the effective Hamiltonian and the Lindblad dissipators, (*i.e.*, coherent and dissipative coupling³⁰). The cross terms in the Lindblad dissipators capture interference effects between different decay channels, as the coupled modes dissipate into the same bath. Such cross terms were also derived for a Jaynes-Cummings model where both the QE and the cavity mode dissipate into the same bath, leading to coupled dissipators between the QE and mode operators to describe Fano-like effects⁹⁰.

To describe the coupling of the modes to a fixed QE at $\mathbf{r}_{\text{QE}} \in \Omega \setminus \Omega_{\text{PML}}$, modeled as a TLS with eigenstates $|g\rangle$, $|e\rangle$ and electric or magnetic transition dipole moment $\mathbf{d}/\mathbf{m} = \langle g | \hat{\mathbf{d}}/\hat{\mathbf{m}} | e \rangle$, the mQED Hamiltonian \hat{H}_{EM} in Eq. (29) would have to be supplemented by additional terms,

$$\begin{aligned} \hat{H} = \hat{H}_{\text{EM}} + \hat{H}_{\text{QE}} + \hat{H}_{\text{int}} \\ = \hat{H}_{\text{EM}} + \hbar \omega_{\text{QE}} \sigma^+ \sigma^- - \hat{\mathbf{d}} \cdot \hat{\mathbf{E}}(\mathbf{r}_{\text{QE}}) - \hat{\mathbf{m}} \cdot \hat{\mathbf{B}}(\mathbf{r}_{\text{QE}}), \end{aligned} \quad (73)$$

in which $\sigma^\pm = |e\rangle\langle g| + |g\rangle\langle e|$ are the usual TLS raising and lowering operators. Note that whilst we treat both possibilities in Eq. (73) for completeness, the distinct selection rules pertaining to electric and magnetic dipole transitions will ensure that only one of \mathbf{d} or \mathbf{m} is non-zero in a given physical application. By using the modal

expansion of the electric field operator in Eq. (50) and following the same steps as before, the master equation thereby obtained possesses the same form as in Eq. (70), but with an effective Hamiltonian

$$\begin{aligned}\hat{H}_{\text{eff}} &= \hbar\omega_{\text{QE}}\sigma^+\sigma^- \\ &+ \hbar\chi_{nn'}^{\lambda,\text{L},+}\hat{a}_{n,\lambda,\text{L}}^\dagger\hat{a}_{n',\lambda,\text{L}} - \hbar\chi_{nn'}^{\lambda,\text{G},+}\hat{a}_{n,\lambda,\text{G}}^\dagger\hat{a}_{n',\lambda,\text{G}} \\ &+ \hbar(g_{n,\lambda,\text{L}}\sigma^+\hat{a}_{n,\lambda,\text{L}} + \text{h.c.}) + \hbar(g_{n,\lambda,\text{G}}\sigma^+\hat{a}_{n,\lambda,\text{G}}^\dagger + \text{h.c.}) ,\end{aligned}\quad (74)$$

where

$$g_{n,\lambda,X} = -\frac{1}{\hbar}(\mathbf{d} \cdot \tilde{\mathbf{E}}_{n,\lambda,X}^{\text{sym}}(\mathbf{r}_{\text{QE}}) + \mathbf{m} \cdot \tilde{\mathbf{B}}_{n,\lambda,X}^{\text{sym}}(\mathbf{r}_{\text{QE}})) ,\quad (75)$$

and we have applied the rotating-wave approximation. It can be appreciated that the gain modal creation operators $\hat{a}_{n,\lambda,\text{G}}^\dagger$ couple to σ^+ in the rotating-wave approximation since they appear in the positive-frequency parts of the fields in Eqs. (50) and (54). If the QE is subject to additional non-radiative decay channels or dephasing processes, the corresponding dissipators should be added to the master equation in Eq. (70). Fig. 2(a) offers a schematic representation of the quantum description for an exemplary resonator-QE system, based on the master equation in this general setting, where the action of the operators and all the different couplings and decay channels are labeled. Note that even though the master equation does not contain coupled dissipators between the QE and mode operators, as derived in Ref.⁹⁰, it is in principle capable of describing coherent Fano interference effects occurring in the QE decay, as the coupling of the QE with the complete set of modes captures its interaction with the electromagnetic environment completely. Such cross terms would appear if a subset of the modes were traced out, as both the QE and the remaining modes couple to these modes.

If the electric and magnetic modal operators are combined, the derivation of the master equation would proceed in a similar manner as before, with the result having the same form as Eq. (70), but with the replacements $\chi^{\lambda,\text{G},\pm} \rightarrow \chi^{\text{G},\pm}$, $\tilde{\chi}^{\lambda,\text{L},\pm} \rightarrow \chi^{\text{L},\pm}$, $\tilde{\chi}^{\lambda,\text{PML},\pm} \rightarrow \chi^{\text{PML},\pm}$, which are exactly defined as in Eqs. (66)-(69), but with the replacements $P^{\lambda,X} \rightarrow P^X$, $\tilde{P}^{\lambda,\text{L}/\text{PML}} \rightarrow \tilde{P}^{\text{L}/\text{PML}}$.

If additionally the gain and loss operators can be combined, the Heisenberg equation for the combined modal operators \hat{a}_n can be written as

$$\begin{aligned}\frac{d\hat{a}_n}{dt} &= \frac{i}{\hbar} [\hat{H}_{\text{eff}}, \hat{a}_n] - (\tilde{\chi}_{nn'}^{\text{L},-} - \tilde{\chi}_{nn'}^{\text{PML+G},-})\hat{a}_{n'} \\ &+ \hat{F}_{n,\text{L}}(t) + \hat{F}_{n,\text{PML+G}}^\dagger(t) ,\end{aligned}\quad (76)$$

with

$$\hat{H}_{\text{eff}} = \hbar\chi_{nn'}^+\hat{a}_n^\dagger\hat{a}_{n'} ,\quad (77)$$

and the matrices

$$\chi_{nn'}^+ = \frac{1}{2}P_{nn''}^{-\frac{1}{2}}(\tilde{\omega}_{n''} + \tilde{\omega}_{n'''}^*)P_{n''n'''}P_{n'''n'}^{-\frac{1}{2}} ,\quad (78)$$

$$\tilde{\chi}_{nn'}^{\text{L},-} = \frac{i}{2}P_{nn''}^{-\frac{1}{2}}(\tilde{\omega}_{n''} - \tilde{\omega}_{n'''}^*)\tilde{P}_{n''n'''}^{\text{L}}P_{n'''n'}^{-\frac{1}{2}} ,\quad (79)$$

$$\begin{aligned}\tilde{\chi}_{nn'}^{\text{PML+G},-} &= \frac{i}{2}P_{nn''}^{-\frac{1}{2}}(\tilde{\omega}_{n''} - \tilde{\omega}_{n'''}^*) \\ &\cdot (\tilde{P}_{n''n'''}^{\text{PML}} + P_{n''n'''}^{\text{G}})P_{n'''n'}^{-\frac{1}{2}} .\end{aligned}\quad (80)$$

The corresponding master equation thus has the form

$$\frac{d\rho}{dt} = -\frac{i}{\hbar} [H_{\text{eff}}, \hat{a}_n] + \tilde{\chi}_{nn'}^{\text{L},-}D_{nn'}^{\text{L}}\rho + \tilde{\chi}_{nn'}^{\text{PML+G},-}D_{nn'}^{\text{PML+G}}\rho ,\quad (81)$$

in which the dissipators $D_{nn'}^{\text{L}}$, $D_{nn'}^{\text{PML+G}}$ are defined just as in Eqs. (71) and (72), respectively. Now that we have included all the gain components into the loss operators, the gain is completely described by incoherent pumping terms (proportional to $\tilde{\chi}_{nn'}^{\text{PML+G},+}$), rather than negative-energy contributions in the effective Hamiltonian. The coupling constants for the interaction with a QE would have the same form as in Eq. (75), but with the accordingly symmetrized modes $\tilde{\mathbf{E}}_n^{\text{sym}}(\mathbf{r}_{\text{QE}})/\tilde{\mathbf{B}}_n^{\text{sym}}(\mathbf{r}_{\text{QE}})$. A schematic representation of the quantum description in this simplified setting is shown in Fig. 2(b). In the case of a resonator with a Drude-Lorentz permittivity and non-dispersive permeability, we can also immediately use the formula obtained from the classical QNM theory in Eq. (20) to describe the driving of the modes by the classical coherent field $\mathbf{E}_b(\mathbf{r}, t)$. In the quantum description, we would introduce an additional driving term $\hat{H}_{\text{drive}}(t)$ in the effective Hamiltonian given by

$$\hat{H}_{\text{drive}}(t) = i\hbar P_{nn'}^{-\frac{1}{2}}D_{n'}(t)\hat{a}_n^\dagger + \text{h.c.} .\quad (82)$$

V. NUMERICAL EXAMPLE: 1D HALF-OPEN CAVITY

Having presented the general formalism in the preceding sections, we now demonstrate the predictive capabilities of our approach in a simple, 1D example. As schematized in Fig. 3(a), we consider a half-open cavity comprising a homogeneous, diamond sample of relative permittivity $\epsilon = 5.7$ and length $L = 200$ nm, with a perfect electrical conductor boundary placed at $x = 0$ (corresponding to a Dirichlet boundary condition imposed at this point). We assume that the diamond hosts a single QE at some location x_{QE} along the x axis, featuring a pair of levels that are coupled by the electric dipole interaction with the cavity field. Such a QE could be realized in the form of a color center in the diamond lattice, and a variety of such optically active defects have been explored for quantum applications⁹¹. For the purpose of our numerical tests, we shall here consider a QE having the transition energy of a nitrogen-vacancy center, namely

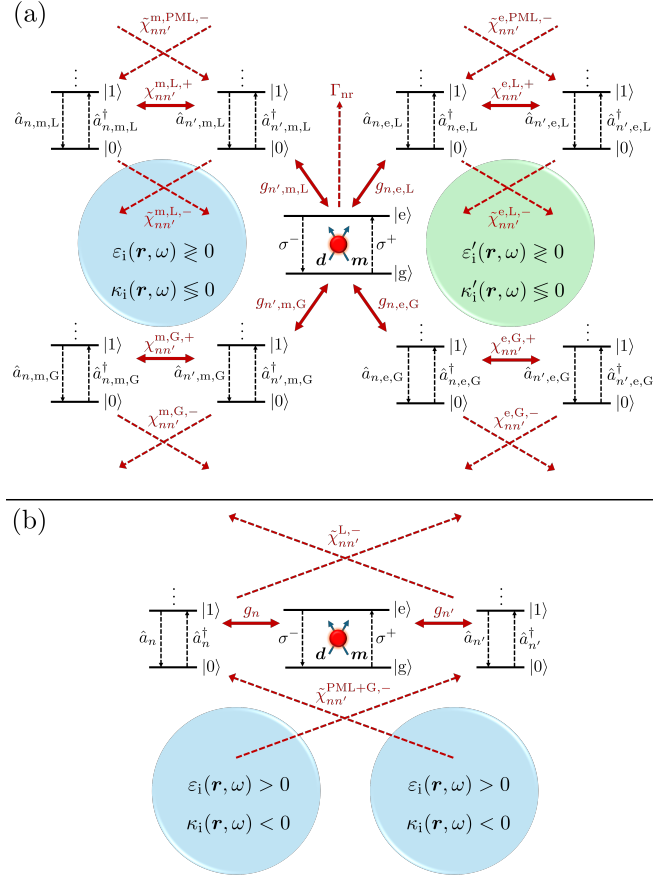


FIG. 2. Schematic representation of the quantum description of an electric/magnetic dipolar QE, modeled as a TLS, interacting with an electromagnetic resonator using PMLs. (a) Most general scenario, in which the resonator could have electric and magnetic gain components in distinct spatial or spectral regions (e.g., a pair of coupled, spherical resonators composed of different materials). In this case, every eigenmode of the resonator (both QNMs and PML modes) is described by four bosonic operators $\hat{a}_{n,\lambda,X}$ with $\lambda = e, m$ and $X = L, G$, corresponding to differently symmetrized modes according to Eqs. (48) and (49). The presence of gain/loss in the system necessitates a symmetrization and the consequent coupling between the symmetrized modes described by $\chi_{nn'}^{\lambda,X,+}$ in the effective Hamiltonian of Eq. (65). The losses of the system are described by Lindblad dissipators proportional to $\tilde{\chi}_{nn'}^{\lambda,L,-}$ and the gain components of the PMLs by incoherent pumping terms proportional to $\tilde{\chi}_{nn'}^{\lambda,PML,-}$, as given in Eqs. (71) and (72), respectively, which also involve coupling between the symmetrized modes. The gain components of the resonator are described by negative-energy contributions in the effective Hamiltonian. All the different bosonic modes couple to the QE with the coupling constants $g_{n,\lambda,X}$, as given in Eq. (75). Additional non-radiative decay or dephasing processes of the QE, here labeled by Γ_{nr} , can be treated in the usual way by adding corresponding Lindblad terms to the master equation. (b) Scenario in which the electric/magnetic and gain/loss modal operators can be combined into a single operator per mode \hat{a}_n (e.g., two spheres composed of passive, magnetodielectric media). In this case, all the gain, both from the PMLs and the resonator, is described by incoherent pumping terms proportional to $\tilde{\chi}_{nn'}^{PML+G,-}$.

$\omega_{QE} = 1.95$ eV (637 nm), and a vertically oriented transition dipole moment \mathbf{d} with controllable magnitude $|\mathbf{d}|$.

A 1D formulation of mQED can be derived for systems that are invariant in two spatial dimensions (say, the y and z directions), and can be used to study the interaction of QEs with linearly polarized radiation propagating in the x direction.⁷³ In this case, we make the replacements $\hat{\mathbf{E}}(\mathbf{r}) \rightarrow \hat{E}(x) = \hat{E}_y(x)$, $\mathbf{d} \rightarrow d = d_y$ and $\hat{f}(\mathbf{r}, \omega) \rightarrow \hat{f}(x, \omega) = \hat{f}_y(x, \omega)$. The y component of the noise current density is then given by

$$\hat{j}_F(x, \omega) = \hat{j}_{F,y}(x, \omega) = \omega \sqrt{\frac{\hbar \varepsilon_0}{\pi A} \tilde{\varepsilon}(x, \omega)} \hat{f}_e(x, \omega) \quad (83)$$

$$+ \partial_x \left(\sqrt{-\frac{\hbar}{\pi \mu_0 A}} \tilde{\kappa}(x, \omega) \hat{f}_m(x, \omega) \right) ,$$

in which A is the normalization area in the yz plane, and we adopt 1D material parameters $\tilde{\zeta}(x, \omega) = \tilde{\zeta}_{yy}(x, \omega)$ appropriate to a single PML in the x direction, given by

$$\tilde{\zeta}(x, \omega) = \zeta(x, \omega) \left(1 + \frac{i}{\omega + i\eta} \sigma_x(x) \right) , \quad (84)$$

as can be obtained from Eqs. (9) and (10) with $\sigma_{y,z} = 0$. In the 1D case, the PMLs are purely lossy, as waves with normal incidence experience only their loss components. In our example, we choose PMLs with a step-like absorption profile, $\sigma_x(x) = 2.5$ eV $\cdot \theta(x - L)$ (i.e., they are directly adjacent to the resonator), a thickness of $20L$ and $\eta = 0.1$ eV. It is worth noting that this 1D problem admits an analytical solution for the QNMs and Green's function directly from the boundary and continuity conditions, thus obviating the need for numerical solution of the 1D Helmholtz equation. As such, spurious numerical reflections that would otherwise arise from a spatial discretization do not occur, and a simple, step-like absorption profile, rather than a gradually increasing one, suffices.

The formulae for the P -matrices all have the same form as in the 3D case, but with the replacements mentioned above and $\nabla \times \rightarrow \partial_x$:

$$P_{nn'} = \frac{\hbar \mu_0}{\pi A} \int_0^\infty d\omega \omega^2 A_n(\omega) A_{n'}^*(\omega) \quad (85)$$

$$\int ds \frac{\omega^2}{c^2} \tilde{\varepsilon}_i(s, \omega) \tilde{E}_n(s) \tilde{E}_{n'}^*(s) - \tilde{\kappa}_i(s, \omega) \partial_s \tilde{E}_n(s) \partial_s \tilde{E}_{n'}^*(s) ,$$

where we have combined the electric and magnetic modal operators. The corresponding master equation then has the same form as in Eq. (81) with $\tilde{\chi}_{nn'}^{PML+G,-} = 0$ and $\tilde{P}_{nn'}^L = P_{nn'}$. In the weak coupling or bad cavity limit, the electromagnetic modes can be traced out to obtain a reduced master equation for the QE only, as was done in Refs.^{54,92}, with the QE decay rate

$$\Gamma_{QE} = \frac{1}{\hbar^2} \Re \left(g_n P_{nn'}^{+\frac{1}{2}} \frac{1}{i(\omega_{QE} - \tilde{\omega}_{n'}^*)} P_{n'n''}^{-\frac{1}{2}} g_{n''}^* \right) . \quad (86)$$

Normalizing this result with respect to the free-space decay rate in 1D, $\Gamma_0 = \omega_{\text{QE}}|d|^2/2\hbar n_b \varepsilon_0 c A$, yields the Purcell factor.

For our calculations using Eq. (86), we retain the three lowest-order QNMs of the resonator which lie in spectral proximity to the QE transition $\omega_{\text{QE}} = 1.95 \text{ eV}$, with complex frequencies $\tilde{\omega}_1 = (0.649 - 0.184i) \text{ eV}$, $\tilde{\omega}_2 = (1.95 - 0.184i) \text{ eV}$ (*i.e.*, resonant with the QE transition) and $\tilde{\omega}_3 = (3.25 - 0.184i) \text{ eV}$, as shown in the upper panel of Fig. 3(b). These modes have very low quality factors of $Q_1 = 1.76$, $Q_2 = 5.28$ and $Q_3 = 8.80$. Furthermore, we assume that the QE is located at $x_{\text{QE}} = 66 \text{ nm}$, where an electric-field antinode of the second-order QNM occurs [see Fig. 3(a)]. Under these conditions, whilst all three QNMs of the resonator offer polarization matching, only the second-order QNM allows optimal spectral and spatial matching with the QE transition. Fig. 3(b) presents our calculated Purcell factor, which bears the expected structure comprising three Lorentzian-like peaks at the spectral locations of the QNMs. In the weak coupling regime considered here, the decay rate can be derived semi-classically using Fermi's golden rule and the Green's function of the electric field⁹³, yielding (in 1D) $\Gamma_{\text{QE}}^{\text{SC}} = \omega_{\text{QE}}^2 |d|^2 \text{Im}(G(x_{\text{QE}}, x_{\text{QE}}, \omega_{\text{QE}})) / \hbar \varepsilon_0 c^2 A$. The predictions obtained using the fully quantum and semi-classical models are compared in the lower panel of Fig. 3(b), showing excellent agreement. Note that we have considered only a finite frequency interval $[\omega_{\text{min}}, \omega_{\text{max}}]$ for the numerical integration in Eq. (85), with $\omega_{\text{min}} = 0.25 \text{ eV}$ and $\omega_{\text{max}} = 4.0 \text{ eV}$.

In the next step, we compare the electric field and QE dynamics in the strong coupling regime. In Ref.^{76,94}, the spontaneous decay of QEs was studied within the framework of mQED. If the QE is prepared in the excited state $|e\rangle$ at time $t = 0$, and the electromagnetic field in the vacuum state $|0\rangle$, then the time-dependent state vector of the system can be written as $|\psi(t)\rangle = C_e(t) e^{-i\omega_{\text{QE}}t} |e\rangle |0\rangle + \int dx \int d\omega C_{g,\lambda}(x, \omega, t) e^{-i\omega t} |g\rangle \hat{f}_\lambda^\dagger(x, \omega) |0\rangle$. From the Heisenberg equations of mQED, an integral equation for the time-dependent coefficient $C_e(t)$ can be derived:

$$C_e(t) = 1 + \int_0^t d\tau K(t - \tau) C_e(\tau), \quad (87)$$

with the kernel

$$K(t - \tau) = \frac{|d|^2}{\hbar \varepsilon_0 \pi A} \int_{\omega_{\text{min}}}^{\omega_{\text{max}}} d\omega \frac{\omega^2}{c^2} \frac{\Im(G(x_{\text{QE}}, x_{\text{QE}}, \omega))}{i(\omega - \omega_{\text{QE}})} \cdot \left(e^{-i(\omega - \omega_{\text{QE}})(t - \tau)} - 1 \right). \quad (88)$$

This equation is derived from the exact mQED formulation and involves no approximations beyond the rotating-wave one for the interaction with the QE. We have solved the integral equation numerically, considering once more a QE tuned to the second-order QNM (*i.e.*,

$\omega_{\text{QE}} = 1.95 \text{ eV}$) and setting the dimensionless dipole moment to be $|d|/\sqrt{\hbar \varepsilon_0 c A} = 0.3$, which although unrealistically high, serves to demonstrate the validity of our theory in the strong coupling case. The result for the occupation probability of the excited state, $|C_e(t)|^2$, can then be compared to the expectation value $\langle \sigma^+(t) \sigma^-(t) \rangle$, obtained from the quantum QNM master equation that we solve using the QuTiP library⁹⁵. The numerical data are plotted in Fig. 4(a), evidencing excellent agreement between the exact theory and the quantum QNM approach in capturing the temporal Rabi oscillations characteristic of this coupling regime. We have further plotted the expectation values of the QNM number operators $\langle \hat{a}_n^\dagger(t) \hat{a}_n(t) \rangle$; as expected, the symmetrized, second-order mode is dominant and undergoes coherent energy exchange with the QE, as reflected in the Rabi oscillations. Moreover, the amplitudes decrease in an approximately linear fashion on the logarithmic plot, with a gradient corresponding to the (equal) imaginary parts of the QNM frequencies $\Im(\tilde{\omega}_n) = -0.184 \text{ eV}$. After the first Rabi oscillation, the other two symmetrized modes show qualitatively similar oscillations as the second-order one, which might be explained by the contribution of the second-order QNM in the other symmetrized modes. Prior to this (*i.e.*, during the first $\sim 10 \text{ fs}$), their dynamics is more complicated and shows additional structure caused by the excitation of the first- and third-order QNMs.

From the exact mQED formulation, one can further derive an equation for the expectation value of the electric field intensity emitted via the spontaneous decay of the QE⁷⁶:

$$\langle \hat{E}^{(-)}(x, t) \hat{E}^{(+)}(x, t) \rangle = \left| \frac{d}{\pi \varepsilon_0 c^2 \sqrt{A}} \int_0^t d\tau C_e(\tau) \cdot \int_{\omega_{\text{min}}}^{\omega_{\text{max}}} d\omega \omega^2 \Im(G(x, x_{\text{QE}}, \omega_{\text{QE}})) e^{-i(\omega - \omega_{\text{QE}})(t - \tau)} \right|^2. \quad (89)$$

In Fig. 4(b), we compare the exact result for the normalized output intensity at $x = L$ with that obtained from the QNM master equation; once again, very good agreement can be seen. We observe two peaks of the intensity attributable to the Rabi oscillations of the second-order mode around $\sim 5 \text{ fs}$ and $\sim 17 \text{ fs}$. However, the first peak has additional substructure. Its maximum is split into a pair of maxima and the second derivative is changing sign along the drop of the peak. For comparison, we plot the intensity calculated from the quantum QNM model upon neglecting the first- and third-order modes (*i.e.*, $|\tilde{E}_2^{\text{sym}}(x)|^2 \langle \hat{a}_2^\dagger(t) \hat{a}_2(t) \rangle$). From this, we can appreciate that the additional substructure originates from a multi-mode effect, as the intensity in this case only displays the two peaks from the Rabi oscillations.

Collectively, our results show that the derived master equation correctly reproduces the dynamics of the QE and electric field, seeding confidence in its application to more complex, quantum nanophotonic systems.

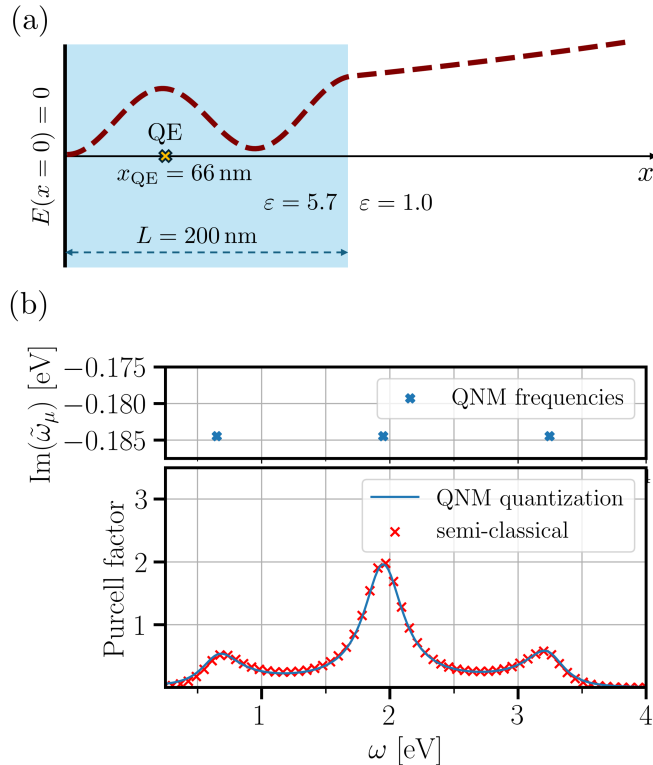


FIG. 3. Numerical exploration of a 1D, half-open, diamond cavity in air, with an electric-dipole QE embedded therein. (a) Schematic of the cavity-QE system with characteristic parameters indicated. The dashed line shows the electric field intensity profile of the second-order QNM, to which the QE is resonantly coupled. (b) Complex frequencies $\tilde{\omega}_n$ of the three, lowest-order QNMs (upper panel) and the frequency-dependent Purcell factor of a QE with $\omega_{QE} = 1.95$ eV (637 nm), calculated in accordance with the quantum QNM and semi-classical theories (lower panel).

It is noteworthy that in this 1D example, we can place the PMLs directly at the open end of the resonator. Positioning the PMLs away from the open end would degrade the accuracy of the results, and increasingly so the farther away they are shifted, given the divergence and incompleteness of the QNMs outside the resonator. In such circumstances, a correct expansion of the Green's function in this region would necessitate taking the PML modes into account. For 3D systems, where there is a transition between the near-field and the divergent far-field regions, optimizing the separation between the resonator and PMLs should aid in reducing the required number of PML modes, a matter to be investigated in greater detail in future studies.

VI. CONCLUSION

In conclusion, we have introduced a formalism for the quantization of QNMs in the presence of 3D, spatially inhomogeneous, dissipative (with possible gain), linear

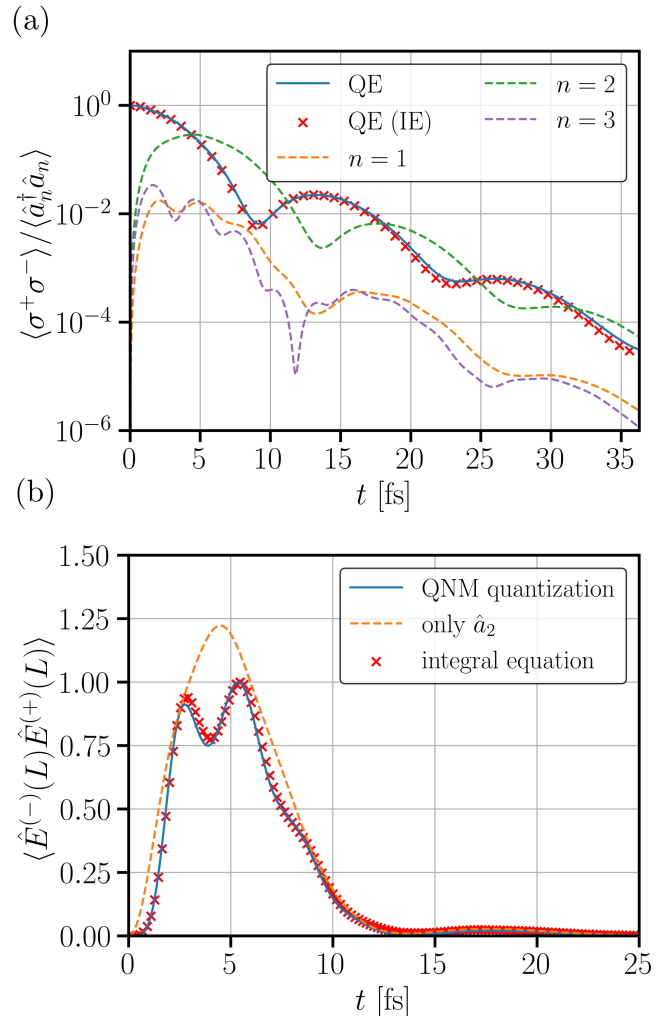


FIG. 4. Spontaneous decay of a QE with $\omega_{QE} = 1.95$ eV and $|d|/\sqrt{\hbar\epsilon_0cA} = 0.3$ in the 1D, half-open cavity of Fig. 3(a). (a) QE and symmetrized mode dynamics obtained by solving the QNM master equation, compared to the QE dynamics obtained from the integral equation Eq. (87) in mQED. (b) Normalized output electric field intensity at $x = L$ obtained from the QNM master equation, compared to the exact mQED result from Eq. (89). Also shown is the electric field intensity calculated from the quantum QNM model retaining only the second-order mode \hat{a}_2 .

magnetodielectric media, enabling a unified and rigorous approach for simulating photonic, plasmonic and magnonic cQED phenomena. Similar to a number of recent works^{54,58,59}, our approach is rooted in the phenomenological Green's function quantization scheme of mQED, but relies on the use of PMLs to achieve a set of modes that are rigorously regularized, orthogonalized and complete, rendering them suitable for the representation of the dyadic Green's function and electromagnetic fields both inside and outside the resonator volume. The introduction of PMLs transforms the radiative losses into non-radiative material dissipation, and via a suitable transformation that reflects all the losses of the resonator,

we are able to define creation and annihilation operators that allow the construction of modal Fock states for the joint excitations of field-dressed matter. Our quantized description of the QNMs thereby provides the foundations for a quantum dynamic treatment of magnetodielectric cQED systems, utilizing discrete modes together with rigorously derived quantum Langevin and master equations. By directly addressing the intricacies of modal loss in a fully quantum theory of magnetodielectric cQED, our approach enables a proper assessment of the performance metrics for nanophotonic device protocols in the Quantum 2.0 era, extending from on-demand sources of single photons, plasmons and magnons, dynamic entanglement generation and quantum state transduction, to light-matter strong coupling in hybrid configurations. Moreover, our quantum QNM theory could prove especially valuable in revealing the opportunities that dissipation may offer in manipulating and tailoring the dynamics of quantum systems (contrary to its traditionally perceived adversarial role), such as in the development of quantum technologies based on quantum nanoplasmonic coherent perfect absorption⁹⁶, non-hermitian topological magnonics³¹ and dissipative photonic time crystals^{97–99}. Note that although the modification of mQED in the case of time-dependent material properties is not trivial, important first steps have very recently been made with the proposition of an mQED Lagrangian for a time-dependent Drude model¹⁰⁰, following the quantization of the electromagnetic field in lossless systems¹⁰¹.

ACKNOWLEDGMENTS

The authors gratefully acknowledge funding from Research Ireland via Grants No. 18/RP/6236 and 22/QERA/3821.

DATA AVAILABILITY STATEMENT

The data that support the findings of this study are available from the corresponding author upon reasonable request.

- ¹K. J. Vahala, “Optical microcavities,” *Nature* **424**, 839–846 (2003).
- ²G. Khitrova, H. M. Gibbs, M. Kira, S. W. Koch, and A. Scherer, “Vacuum rabi splitting in semiconductors,” *Nature Physics* **2**, 81–90 (2006).
- ³M. Kira and S. W. Koch, *Semiconductor Quantum Optics* (Cambridge University Press, 2011).
- ⁴S. Hepp, M. Jetter, S. L. Portalupi, and P. Michler, “Semiconductor quantum dots for integrated quantum photonics,” *Advanced Quantum Technologies* **2**, 1900020 (2019).
- ⁵Y. Arakawa and M. J. Holmes, “Progress in quantum-dot single photon sources for quantum information technologies: A broad spectrum overview,” *Applied Physics Reviews* **7**, 021309 (2020).
- ⁶T. Heindel, J.-H. Kim, N. Gregersen, A. Rastelli, and S. Reitzenstein, “Quantum dots for photonic quantum information technology,” *Adv. Opt. Photon.* **15**, 613–738 (2023).

- ⁷J. J. Baumberg, J. Aizpurua, M. H. Mikkelsen, and D. R. Smith, “Extreme nanophotonics from ultrathin metallic gaps,” *Nature materials* **18**, 668–678 (2019).
- ⁸R. Chikkaraddy, B. De Nijs, F. Benz, S. J. Barrow, O. A. Scherman, E. Rosta, A. Demetriadou, P. Fox, O. Hess, and J. J. Baumberg, “Single-molecule strong coupling at room temperature in plasmonic nanocavities,” *Nature* **535**, 127–130 (2016).
- ⁹K. Santhosh, O. Bitton, L. Chuntonov, and G. Haran, “Vacuum rabi splitting in a plasmonic cavity at the single quantum emitter limit,” *Nature Communications* **7**, ncomms11823 (2016).
- ¹⁰H. Groß, J. M. Hamm, T. Tufarelli, O. Hess, and B. Hecht, “Near-field strong coupling of single quantum dots,” *Science Advances* **4**, eaar4906 (2018).
- ¹¹K.-D. Park, M. A. May, H. Leng, J. Wang, J. A. Kropp, T. Gougousi, M. Pelton, and M. B. Raschke, “Tip-enhanced strong coupling spectroscopy, imaging, and control of a single quantum emitter,” *Science Advances* **5**, eaav5931 (2019).
- ¹²X. Xiong, N. Kongsuwan, Y. Lai, C. E. Png, L. Wu, and O. Hess, “Room-temperature plexcitonic strong coupling: Ultrafast dynamics for quantum applications,” *Applied Physics Letters* **118**, 130501 (2021).
- ¹³D. D. A. Clarke and O. Hess, “Near-field strong coupling and entanglement of quantum emitters for room-temperature quantum technologies,” *PhotoniX* **5**, 33 (2024).
- ¹⁴Y. Zhang, Q.-S. Meng, L. Zhang, Y. Luo, Y.-J. Yu, B. Yang, Y. Zhang, R. Esteban, J. Aizpurua, Y. Luo, J.-L. Yang, Z.-C. Dong, and J. G. Hou, “Sub-nanometre control of the coherent interaction between a single molecule and a plasmonic nanocavity,” *Nature Communications* **8**, 15225 (2017).
- ¹⁵T. B. Hoang, G. M. Akselrod, and M. H. Mikkelsen, “Ultrafast room-temperature single photon emission from quantum dots coupled to plasmonic nanocavities,” *Nano Letters* **16**, 270–275 (2016).
- ¹⁶S. I. Bogdanov, O. A. Makarova, X. Xu, Z. O. Martin, A. S. Lagutchev, M. Olinde, D. Shah, S. N. Chowdhury, A. R. Gabidullin, I. A. Ryzhikov, I. A. Rodionov, A. V. Kildishev, S. I. Bozhevolnyi, A. Boltasseva, V. M. Shalaev, and J. B. Khurgin, “Ultrafast quantum photonics enabled by coupling plasmonic nanocavities to strongly radiative antennas,” *Optica* **7**, 463–469 (2020).
- ¹⁷J.-B. You, X. Xiong, P. Bai, Z.-K. Zhou, R.-M. Ma, W.-L. Yang, Y.-K. Lu, Y.-F. Xiao, C. E. Png, F. J. Garcia-Vidal, C.-W. Qiu, and L. Wu, “Reconfigurable photon sources based on quantum plexcitonic systems,” *Nano Letters* **20**, 4645–4652 (2020).
- ¹⁸F. Bello, N. Kongsuwan, J. F. Donegan, and O. Hess, “Controlled cavity-free, single-photon emission and bipartite entanglement of near-field-excited quantum emitters,” *Nano Letters* **20**, 5830–5836 (2020).
- ¹⁹F. D. Bello, N. Kongsuwan, and O. Hess, “Near-field generation and control of ultrafast, multipartite entanglement for quantum nanoplasmonic networks,” *Nano Letters* **22**, 2801–2808 (2022).
- ²⁰N. Kongsuwan, X. Xiong, P. Bai, J.-B. You, C. E. Png, L. Wu, and O. Hess, “Quantum plasmonic immunoassay sensing,” *Nano Letters* **19**, 5853–5861 (2019).
- ²¹X. Zhang, C.-L. Zou, L. Jiang, and H. X. Tang, “Strongly coupled magnons and cavity microwave photons,” *Phys. Rev. Lett.* **113**, 156401 (2014).
- ²²J. T. Hou and L. Liu, “Strong coupling between microwave photons and nanomagnet magnons,” *Phys. Rev. Lett.* **123**, 107702 (2019).
- ²³Y. Li, T. Polakovic, Y.-L. Wang, J. Xu, S. Lendinez, Z. Zhang, J. Ding, T. Khaire, H. Saglam, R. Divan, J. Pearson, W.-K. Kwok, Z. Xiao, V. Novosad, A. Hoffmann, and W. Zhang, “Strong coupling between magnons and microwave photons in on-chip ferromagnet-superconductor thin-film devices,” *Phys. Rev. Lett.* **123**, 107701 (2019).
- ²⁴T. Neuman, D. S. Wang, and P. Narang, “Nanomagnonic cavities for strong spin-magnon coupling and magnon-mediated spin-spin interactions,” *Phys. Rev. Lett.* **125**, 247702 (2020).

²⁵B. Z. Rameshti, S. V. Kusminskiy, J. A. Haigh, K. Usami, D. Lachance-Quirion, Y. Nakamura, C.-M. Hu, H. X. Tang, G. E. Bauer, and Y. M. Blanter, "Cavity magnonics," *Physics Reports* **979**, 1–61 (2022).

²⁶A. Gardin, G. Bourcin, J. Bourhill, V. Vlaminck, C. Person, C. Fumeaux, G. C. Tettamanzi, and V. Castel, "Engineering synthetic gauge fields through the coupling phases in cavity magnonics," *Physical Review Applied* **21**, 064033 (2024).

²⁷K. C. Chen, I. Christen, H. Raniwala, M. Colangelo, L. De Santis, K. Shtyrkova, D. Starling, R. Murphy, L. Li, K. Berggren, *et al.*, "A scalable cavity-based spin–photon interface in a photonic integrated circuit," *Optica Quantum* **2**, 124–132 (2024).

²⁸P. T. Kristensen, C. V. Vlack, and S. Hughes, "Generalized effective mode volume for leaky optical cavities," *Opt. Lett.* **37**, 1649–1651 (2012).

²⁹P. T. Kristensen and S. Hughes, "Modes and mode volumes of leaky optical cavities and plasmonic nanoresonators," *ACS Photonics* **1**, 2–10 (2014).

³⁰Y.-P. Wang and C.-M. Hu, "Dissipative couplings in cavity magnonics," *Journal of Applied Physics* **127**, 130901 (2020).

³¹T. Yu, J. Zou, B. Zeng, J. Rao, and K. Xia, "Non-hermitian topological magnonics," *Physics Reports* **1062**, 1–86 (2024), non-Hermitian topological magnonics.

³²H. M. Lai, P. T. Leung, K. Young, P. W. Barber, and S. C. Hill, "Time-independent perturbation for leaking electromagnetic modes in open systems with application to resonances in microdroplets," *Phys. Rev. A* **41**, 5187–5198 (1990).

³³P. T. Leung, S. Y. Liu, and K. Young, "Completeness and orthogonality of quasinormal modes in leaky optical cavities," *Phys. Rev. A* **49**, 3057–3067 (1994).

³⁴P. T. Leung, S. Y. Liu, S. S. Tong, and K. Young, "Time-independent perturbation theory for quasinormal modes in leaky optical cavities," *Phys. Rev. A* **49**, 3068–3073 (1994).

³⁵P. T. Leung and K. M. Pang, "Completeness and time-independent perturbation of morphology-dependent resonances in dielectric spheres," *J. Opt. Soc. Am. B* **13**, 805–817 (1996).

³⁶K. M. Lee, P. T. Leung, and K. M. Pang, "Dyadic formulation of morphology-dependent resonances. i. completeness relation," *J. Opt. Soc. Am. B* **16**, 1409–1417 (1999).

³⁷W. Yan, R. Faggiani, and P. Lalanne, "Rigorous modal analysis of plasmonic nanoresonators," *Phys. Rev. B* **97**, 205422 (2018).

³⁸P. Lalanne, W. Yan, K. Vynck, C. Sauvan, and J.-P. Hugonin, "Light interaction with photonic and plasmonic resonances," *Laser & Photonics Reviews* **12**, 1700113 (2018).

³⁹C. Sauvan, T. Wu, R. Zarouf, E. A. Muljarov, and P. Lalanne, "Normalization, orthogonality, and completeness of quasinormal modes of open systems: the case of electromagnetism [invited]," *Opt. Express* **30**, 6846–6885 (2022).

⁴⁰Q. Bai, M. Perrin, C. Sauvan, J.-P. Hugonin, and P. Lalanne, "Efficient and intuitive method for the analysis of light scattering by a resonant nanostructure," *Opt. Express* **21**, 27371–27382 (2013).

⁴¹C. Sauvan, J. P. Hugonin, I. S. Maksymov, and P. Lalanne, "Theory of the spontaneous optical emission of nanosize photonic and plasmon resonators," *Phys. Rev. Lett.* **110**, 237401 (2013).

⁴²R.-C. Ge and S. Hughes, "Design of an efficient single photon source from a metallic nanorod dimer: a quasi-normal mode finite-difference time-domain approach," *Opt. Lett.* **39**, 4235–4238 (2014).

⁴³R.-C. Ge, P. T. Kristensen, J. F. Young, and S. Hughes, "Quasinormal mode approach to modelling light-emission and propagation in nanoplasmatics," *New Journal of Physics* **16**, 113048 (2014).

⁴⁴T. Wu, D. Arrivault, W. Yan, and P. Lalanne, "Modal analysis of electromagnetic resonators: User guide for the man program," *Computer Physics Communications* **284**, 108627 (2023).

⁴⁵N. Kongsuwan, A. Demetriadou, M. Horton, R. Chikkaraddy, J. J. Baumberg, and O. Hess, "Plasmonic nanocavity modes: From near-field to far-field radiation," *ACS Photonics* **7**, 463–471 (2020).

⁴⁶J. Ren, S. Franke, A. Knorr, M. Richter, and S. Hughes, "Near-field to far-field transformations of optical quasinormal modes and efficient calculation of quantized quasinormal modes for open cavities and plasmonic resonators," *Phys. Rev. B* **101**, 205402 (2020).

⁴⁷K. Bedingfield, E. Elliott, A. Gisdakis, N. Kongsuwan, J. J. Baumberg, and A. Demetriadou, "Multi-faceted plasmonic nanocavities," *Nanophotonics* **12**, 3931–3944 (2023).

⁴⁸M. Kamandar Dezfooli, R. Gordon, and S. Hughes, "Modal theory of modified spontaneous emission of a quantum emitter in a hybrid plasmonic photonic-crystal cavity system," *Phys. Rev. A* **95**, 013846 (2017).

⁴⁹J. Ren, S. Franke, B. VanDrunen, and S. Hughes, "Classical purcell factors and spontaneous emission decay rates in a linear gain medium," *Phys. Rev. A* **109**, 013513 (2024).

⁵⁰A.-W. El-Sayed and S. Hughes, "Quasinormal-mode theory of elastic purcell factors and fano resonances of optomechanical beams," *Phys. Rev. Res.* **2**, 043290 (2020).

⁵¹T. Neuman, J. Aizpurua, and R. Esteban, "Quantum theory of surface-enhanced resonant raman scattering (serrs) of molecules in strongly coupled plasmon–exciton systems," *Nanophotonics* **9**, 295–308 (2020).

⁵²V. D. Giulio, M. Kociak, and F. J. G. de Abajo, "Probing quantum optical excitations with fast electrons," *Optica* **6**, 1524–1534 (2019).

⁵³W.-J. Zhou, J. bin You, X. Xiong, Y.-W. Lu, L. K. Ang, J.-F. Liu, and L. Wu, "Cavity spectral-hole-burning to boost coherence in plasmon-emitter strong coupling systems," *Nanotechnology* **33**, 475001 (2022).

⁵⁴S. Franke, S. Hughes, M. K. Dezfooli, P. T. Kristensen, K. Busch, A. Knorr, and M. Richter, "Quantization of quasinormal modes for open cavities and plasmonic cavity quantum electrodynamics," *Phys. Rev. Lett.* **122**, 213901 (2019).

⁵⁵S. Hughes, S. Franke, C. Gustin, M. Kamandar Dezfooli, A. Knorr, and M. Richter, "Theory and limits of on-demand single-photon sources using plasmonic resonators: A quantized quasinormal mode approach," *ACS Photonics* **6**, 2168–2180 (2019).

⁵⁶S. Franke, M. Richter, J. Ren, A. Knorr, and S. Hughes, "Quantized quasinormal-mode description of nonlinear cavity-qed effects from coupled resonators with a fano-like resonance," *Phys. Rev. Res.* **2**, 033456 (2020).

⁵⁷S. Franke, J. Ren, and S. Hughes, "Quantized quasinormal-mode theory of coupled lossy and amplifying resonators," *Phys. Rev. A* **105**, 023702 (2022).

⁵⁸I. Medina, F. J. García-Vidal, A. I. Fernández-Domínguez, and J. Feist, "Few-mode field quantization of arbitrary electromagnetic spectral densities," *Phys. Rev. Lett.* **126**, 093601 (2021).

⁵⁹J. Feist, A. I. Fernández-Domínguez, and F. J. García-Vidal, "Macroscopic qed for quantum nanophotonics: emitter-centered modes as a minimal basis for multiemitter problems," *Nanophotonics* **10**, 477–489 (2020).

⁶⁰B. Yuen and A. Demetriadou, "Exact quantum electrodynamics of radiative photonic environments," *Physical Review Letters* **133**, 203604 (2024).

⁶¹F. Binder, L. A. Correa, C. Gogolin, J. Anders, and G. Adesso, "Thermodynamics in the quantum regime," *Fundamental Theories of Physics* **195** (2018).

⁶²N. Anto-Sztrikacs and D. Segal, "Capturing non-markovian dynamics with the reaction coordinate method," *Physical Review A* **104**, 052617 (2021).

⁶³J. P. Hugonin and P. Lalanne, "Perfectly matched layers as nonlinear coordinate transforms: a generalized formalization," *J. Opt. Soc. Am. A* **22**, 1844–1849 (2005).

⁶⁴G. Deméy, T. Wu, Y. Brûlé, F. Zolla, A. Nicolet, P. Lalanne, and B. Gralak, "Dispersive perfectly matched layers and high-order absorbing boundary conditions for electromagnetic quasinormal modes," *J. Opt. Soc. Am. A* **40**, 1947–1958 (2023).

⁶⁵P. T. Kristensen, J. R. de Lasson, and N. Gregersen, "Calculation, normalization, and perturbation of quasinormal modes in coupled cavity-waveguide systems," *Optics Letters* **39**, 6359–6362 (2014).

⁶⁶P. T. Kristensen, J. R. De Lasson, M. Heuck, N. Gregersen, and J. Mørk, "On the theory of coupled modes in optical cavity-waveguide structures," *Journal of Lightwave Technology* **35**, 4247–4259 (2017).

⁶⁷Notably however, static/longitudinal modes with $\tilde{\omega}_\mu = 0 \in \mathbb{R}$ can occur, and the significance of their non-resonant contribution in QNM theories has been investigated in the literature^{82,102}.

⁶⁸J.-P. Berenger, "A perfectly matched layer for the absorption of electromagnetic waves," *Journal of computational physics* **114**, 185–200 (1994).

⁶⁹A. F. Oskooi, L. Zhang, Y. Avniel, and S. G. Johnson, "The failure of perfectly matched layers, and towards their redemp-tion by adiabatic absorbers," *Optics Express* **16**, 11376–11392 (2008).

⁷⁰A. J. Ward and J. B. Pendry, "Refraction and geometry in maxwell's equations," *Journal of modern optics* **43**, 773–793 (1996).

⁷¹F. Olyslager, "Discretization of continuous spectra based on perfectly matched layers," *SIAM Journal on Applied Mathematics* **64**, 1408–1433 (2004).

⁷²P. Lalanne, W. Yan, A. Gras, C. Sauvan, J.-P. Hugonin, M. Besbes, G. Demésy, M. Truong, B. Gralak, F. Zolla, *et al.*, "Quasi-normal mode solvers for resonators with dispersive materials," *Journal of the Optical Society of America A* **36**, 686–704 (2019).

⁷³T. Gruner and D.-G. Welsch, "Green-function approach to the radiation-field quantization for homogeneous and inhomogeneous kramers-kronig dielectrics," *Phys. Rev. A* **53**, 1818–1829 (1996).

⁷⁴H. T. Dung, L. Knöll, and D.-G. Welsch, "Three-dimensional quantization of the electromagnetic field in dispersive and absorbing inhomogeneous dielectrics," *Phys. Rev. A* **57**, 3931–3942 (1998).

⁷⁵S. Scheel, L. Knöll, and D.-G. Welsch, "Qed commutation relations for inhomogeneous kramers-kronig dielectrics," *Phys. Rev. A* **58**, 700–706 (1998).

⁷⁶H. T. Dung, L. Knöll, and D.-G. Welsch, "Spontaneous decay in the presence of dispersing and absorbing bodies: General theory and application to a spherical cavity," *Phys. Rev. A* **62**, 053804 (2000).

⁷⁷C. Raabe, S. Scheel, and D.-G. Welsch, "Unified approach to qed in arbitrary linear media," *Physical Review A—Atomic, Molecular, and Optical Physics* **75**, 053813 (2007).

⁷⁸R. Matloob, R. Loudon, M. Artoni, S. M. Barnett, and J. Jeffers, "Electromagnetic field quantization in amplifying dielectrics," *Physical Review A* **55**, 1623 (1997).

⁷⁹C. Raabe and D.-G. Welsch, "Qed in arbitrary linear media: Amplifying media," *The European Physical Journal Special Topics* **160**, 371–381 (2008).

⁸⁰S. Y. Buhmann, D. T. Butcher, and S. Scheel, "Macroscopic quantum electrodynamics in nonlocal and nonreciprocal media," *New Journal of Physics* **14**, 083034 (2012).

⁸¹M. Kuzuoglu and R. Mittra, "Frequency dependence of the constitutive parameters of causal perfectly matched anisotropic absorbers," *IEEE Microwave and Guided wave letters* **6**, 447–449 (2002).

⁸²M. Besbes and C. Sauvan, "Role of static modes in quasinormal modes expansions: when and how to take them into account?" *Mathematics* **10**, 3542 (2022).

⁸³T. G. Philbin, "Canonical quantization of macroscopic electromagnetism," *New Journal of Physics* **12**, 123008 (2010).

⁸⁴E. Amooghorban, M. Wubs, N. A. Mortensen, and F. Kheirandish, "Casimir forces in multilayer magnetodielectrics with both gain and loss," *Physical Review A—Atomic, Molecular, and Optical Physics* **84**, 013806 (2011).

⁸⁵S. Franke, J. Ren, M. Richter, A. Knorr, and S. Hughes, "Fermi's golden rule for spontaneous emission in absorptive and amplifying media," *Physical Review Letters* **127**, 013602 (2021).

⁸⁶A. Sambale, D. G. Welsch, S. Y. Buhmann, and H. T. Dung, "Casimir force on amplifying bodies," *Optics and Spectroscopy* **108**, 391–399 (2010).

⁸⁷P.-O. Löwdin, "On the non-orthogonality problem connected with the use of atomic wave functions in the theory of molecules and crystals," *The Journal of Chemical Physics* **18**, 365–375 (1950).

⁸⁸S. Franke, J. Ren, S. Hughes, and M. Richter, "Fluctuation-dissipation theorem and fundamental photon commutation relations in lossy nanostructures using quasinormal modes," *Physical Review Research* **2**, 033332 (2020).

⁸⁹C. W. Gardiner and M. J. Collett, "Input and output in damped quantum systems: Quantum stochastic differential equations and the master equation," *Physical Review A* **31**, 3761 (1985).

⁹⁰M. Yamaguchi, A. Lyasota, and T. Yuge, "Theory of fano effect in cavity quantum electrodynamics," *Physical Review Research* **3**, 013037 (2021).

⁹¹I. Aharonovich and E. Neu, "Diamond nanophotonics," *Advanced Optical Materials* **2**, 911–928 (2014).

⁹²J. I. Cirac, "Interaction of a two-level atom with a cavity mode in the bad-cavity limit," *Physical Review A* **46**, 4354 (1992).

⁹³L. Novotny and B. Hecht, *Principles of Nano-Optics* (Cambridge University Press, 2006).

⁹⁴S. Scheel and S. Y. Buhmann, "Macroscopic quantum electrodynamics-concepts and applications," *Acta Phys. Slovaca* **58**, 675–809 (2008).

⁹⁵N. Lambert, E. Giguère, P. Menczel, B. Li, P. Hopf, G. Suárez, M. Gali, J. Lishman, R. Gadhvi, R. Agarwal, *et al.*, "Qutip 5: The quantum toolbox in python," *arXiv preprint arXiv:2412.04705* (2024).

⁹⁶Y. Lai, D. D. A. Clarke, P. Grimm, A. Devi, D. Wigger, T. Helbig, T. Hofmann, R. Thomale, J.-S. Huang, B. Hecht, *et al.*, "Room-temperature quantum nanoplasmionic coherent perfect absorption," *Nature Communications* **15**, 6324 (2024).

⁹⁷M. Lyubarov, Y. Lumer, A. Dikopoltsev, E. Lustig, Y. Sharabi, and M. Segev, "Amplified emission and lasing in photonic time crystals," *Science* **377**, 425–428 (2022).

⁹⁸T. Liu, J.-Y. Ou, K. F. MacDonald, and N. I. Zheludev, "Photonic metamaterial analogue of a continuous time crystal," *Nature Physics* **19**, 986–991 (2023).

⁹⁹J. E. Sustaeta-Osuna, F. J. García-Vidal, and P. A. Huidobro, "Quantum theory of photon pair creation in photonic time crystals," *ACS Photonics* **12**, 1873–1880 (2025).

¹⁰⁰S. Horsley and R. Baker, "Macroscopic qed and noise currents in time-varying media," *Physical Review A* **111**, 053511 (2025).

¹⁰¹J. Pendry and S. A. Horsley, "Qed in space-time varying materials," *APL Quantum* **1** (2024).

¹⁰²C. Sauvan, "Quasinormal modes expansions for nanoresonators made of absorbing dielectric materials: study of the role of static modes," *Optics Express* **29**, 8268–8282 (2021).